

Symmetry Decomposition of Chaotic Dynamics

Predrag Cvitanović

Dept. of Physics, New York University, New York, NY 10003

and

Niels Bohr Institute¹, Blegdamsvej 17, DK-2100 Copenhagen Ø

and

Bruno Eckhardt

Fachbereich Physik der Philipps-Universität,

Renthof 6, D-3550 Marburg

PACS numbers: **05.45.+b**, **03.65 Sq**, **2.20.+b**, **3.20.+i**

Abstract

Discrete symmetries of dynamical flows give rise to relations between periodic orbits, reduce the dynamics to a fundamental domain, and lead to factorizations of zeta functions. These factorizations in turn reduce the labor and improve the convergence of cycle expansions for classical and quantum spectra associated with the flow. In this paper the general formalism is developed, with the N -disk pinball model used as a concrete example and a series of physically interesting cases worked out in detail.

¹ permanent address

1 Introduction

submitted to Nonlinearity Feb 26, 92; revised Oct 19, 92; file printed October 30, 2018

The periodic orbit theory of classical chaotic dynamical systems has a long and distinguished history; initiated by Poincaré[1], and developed as a mathematical theory of hyperbolic dynamical systems by Smale, Sinai, Bowen, Ruelle and others[2, 3, 4, 5], it has in recent years been applied to many systems of physical interest[6, 7, 8, 9]. The periodic orbit theory of quantum mechanical systems largely parallels this development; originating in the work of Hadamard[10] and Selberg[11], it has been developed as a quantum mechanical theory by Gutzwiller, Balian and Bloch, Berry and others[12, 13, 14, 15, 16], and has been in the focus of much recent research. In both the classical and the quantum contexts, one is interested in computing spectra of certain evolution operators; this can be done by determining zeros of Fredholm determinants or associated zeta functions[5, 11, 17]. The periodic orbits emerge in this context essentially through the identity $\log \det = \text{tr} \log$ which relates the spectrum to the traces of the evolution operators, *i.e.*, the periodic orbits or cycles.

As demonstrated in a series of papers [9],[18]-[22], cycle expansions of zeta functions can be profitably used for the calculation of such spectra in chaotic dynamical systems. These systems often come equipped with discrete symmetries, such as the reflection and the rotation symmetries of various potentials. We shall show here that such symmetries simplify and improve the cycle expansions in a rather beautiful way; they can be exploited to relate classes of periodic orbits and factorize zeta functions, not only in quantum mechanics (where the utility of discrete symmetry factorizations is well known[23]), but also in classical mechanics. The group-theoretic factorizations of zeta functions that we develop here were first introduced and applied in ref. [9]. They are closely related to the symmetrizations introduced by Gutzwiller[24] in the context of the semiclassical periodic orbit trace formulas, recently put into more general group-theoretic context by Robbins[25], whose exposition, together with Lauritzen's[26] treatment of the boundary orbits, has influenced the presentation given here. A related group-theoretic decomposition

in context of hyperbolic billiards was utilized in ref. [27].

Invariance of a system under symmetries means that the symmetry image of a cycle is again a cycle, with the same weight. The new orbit may be topologically distinct (in which case it contributes to the multiplicity of the cycle) or it may be the same cycle, shifted in time. In the latter case, the cycle can be subdivided into segments, each of which is a symmetry image of an irreducible segment. The period or the action of the full orbit is given by the sum along the segments, whereas the stability is given by the product of the stability matrices of the individual segments. The phase space can be completely tiled by a fundamental domain and its symmetry images (“phase space” in this paper stands for the coordinates of any d -dimensional dynamical system whose evolution is described by a set of first order differential equations or iterative mappings, not necessarily Hamiltonian). The irreducible segments of cycles in the full space, folded back into the fundamental domain, are closed orbits in the reduced space.

The main point of this paper is that if the dynamics possesses a discrete symmetry, the contribution of a cycle p of multiplicity m_p to a dynamical zeta function *factorizes* into a product over the d_α -dimensional irreducible representations D_α of the symmetry group,

$$(1 - t_p)^{m_p} = \prod_{\alpha} \det(1 - D_{\alpha}(h)_{\tilde{p}} t_{\tilde{p}})^{d_{\alpha}}, \quad t_p = t_{\tilde{p}}^{g/m_p}, \quad (1)$$

where $t_{\tilde{p}}$ is the cycle weight evaluated on the fundamental domain, g is the dimension of the group, $h_{\tilde{p}}$ is the group element relating the fundamental domain cycle \tilde{p} to a segment of the full space cycle p , and m_p is the multiplicity of the p cycle. Emergence of symmetrized subspaces, a common phenomenon in quantum mechanics, is perhaps surprising in a classical dynamics context. The basic idea is simple: in classical dynamics, just as in quantum mechanics, the symmetrized subspaces can be probed by linear operators (observables) of different symmetries. If a linear operator commutes with the symmetry, it can be block-diagonalized and the associated determinants will therefore factorize.

This paper is meant to serve as a detailed guide to computation of zeta functions for systems with discrete symmetries. We develop here the cycle expansions needed for evaluation of factorized zeta functions, and exemplify them by working out a series of cases of physical interest: C_2, C_{2v}, C_{3v} and C_{4v} symmetries. For instance, one has a C_2 symmetry in the Lorenz system[28, 29], the Ising model, and in the

3-dimensional anisotropic Kepler potential[24, 30, 31], a C_{3v} symmetry in Hénon-Heiles type potentials[32, 33, 34, 26], a C_{4v} symmetry in quartic oscillators[35, 36], in the pure x^2y^2 potential[37, 38] and in hydrogen in a magnetic field[39], and a $C_{2v} = C_2 \times C_2$ symmetry in the stadium billiard[25].

We will illustrate our results using the pinball scattering by three and four disks[40] as an example. Besides their intrinsic interest as examples of classical and quantum mechanical chaotic dynamics[23, 9, 41, 42], they are also relevant to smooth potentials. The pinball model may be thought of as the infinite potential wall limit of a smooth potential, and, much as the 1-d tent map captures the topology of a general unimodal map, the N -disk symbol dynamics can serve as a *covering* symbolic dynamics in smooth potentials. One may either define potential wall collisions in phase space[39, 43] or one may start with the infinite wall limit and continuously relax an unstable cycle onto the corresponding one for the potential under investigation. If things go well, the cycle will remain unstable and isolated, no new orbits (unaccounted for by the N -disk symbolic dynamics) will be born, and the lost orbits will be accounted for by a set of pruning rules. For example, this adiabatic approach has been profitably used in ref. [44] in disproving the conjecture that the x^2y^2 potential is ergodic. Its validity has to be checked carefully in each application, as things can easily go wrong; for example, near bifurcations the same naive symbol string assignments can refer to a whole island of distinct periodic orbits.

In addition to the symmetries exploited here, time reversal symmetry and a variety of other non-trivial discrete symmetries can induce further relations among orbits; we shall point out several of examples of cycle degeneracies under time reversal. We do not know whether such symmetries can be exploited for further improvements of cycle expansions.

The paper is organized as follows. In the next section, we recall some basic facts of the zeta-function formalism and cycle expansions, and describe the symbolic dynamics of the N -disk model. In section 3 we illustrate the utility of zeta function formalism by using it to count cycles. In section 4 we introduce discrete symmetries and apply them to identify degenerate classes of cycles. In section 5 we describe the reduction of the N -disk dynamics to the fundamental domain and the special treatment required by boundary orbits. Finally, in section 6 we apply symmetries to reduce the symbolic dynamics and to factorize zeta functions. Several examples are worked out in detail. Cycle expansions for the (symmetry unreduced) 3- and

4-disk dynamics are listed in the appendix. We conclude with a summary and an outlook for further work.

2 Preliminaries

Here and in sect. 3 we review the cycle expansion formalism; the subject proper of the paper, group-theoretic factorizations, commences only in sect. 4. The reader might profitably start with sect. 4, and refer back to the preliminaries of sects. 2 and 3 as need arises.

2.1 Zeta functions

Transfer operators and the associated zeta functions are treated extensively in the literature[5]. Here we merely state the results needed for the purposes of this paper, in the notation of ref. [18].

The general setting is as follows: given a dynamical system, presented either as a d -dimensional map $f(x)$, or as a $d+1$ dimensional flow (in the latter case, the flow can be reduced to a d -dimensional mapping by means of appropriate Poincaré sections), one is interested in time evolution of certain distributions, such as classical probability distributions and quantum mechanical wave functions. The effect of the dynamics on such distributions is given by linear evolution operators, such as the integral kernel used in evaluation of the escape rate from a repeller[45] described by a map $x_{n+1} = f(x_n)$,

$$\mathcal{L}(y, x) = \delta(y - f(x)) . \tag{2}$$

The time dependence of distributions in question is determined by the eigenspectrum and eigenfunctions of evolution operators, and the problem that concerns us here is the problem of effective evaluation of such eigenspectra for a given dynamical system.

The eigenvalues λ_k of \mathcal{L} are the inverses of the zeros of

$$Z(z) = \text{Det}(1 - z\mathcal{L}) = \prod_{k=0}^{\infty} (1 - z\lambda_k) . \tag{3}$$

The periodic orbit approach to the determination of zeros of $Z(z)$ is based on the observation that the determinant of an operator is related to its traces by

$$\det(1 - z\mathcal{L}) = \exp\left(-\sum_{n=1}^{\infty} \frac{z^n}{n} \operatorname{tr} \mathcal{L}^n\right) \quad (4)$$

Traces of an operator like (2) receive contributions from all prime cycles p of period n_p and their multiple traversals, weighted by the cycle Jacobians

$$Z(z) = \exp\left(-\sum_p \sum_{r=1}^{\infty} \frac{1}{r} \frac{z^{n_p r}}{|\det(\mathbf{1} - \mathbf{J}_p^r)|}\right). \quad (5)$$

This expression for $\operatorname{Det}(1 - z\mathcal{L})$ is specific to the mapping (2). In more general settings[5], z^{n_p} is replaced by a weight whose precise form depends on the particular average being computed; for example, in the corresponding determinant for classical smooth flows, z^{n_p} is replaced by e^{sT_p} , where T_p is the p cycle period[46]. The quantum mechanical kernel corresponding to (2) is smeared out by a path integral, but in the semiclassical approximation[14] the zeta function[17] has essentially the same form as (5):

$$Z(E) = \exp\left(-\sum_p \sum_{r=1}^{\infty} \frac{1}{r} \frac{e^{\frac{i}{\hbar} S_p(E)r - i\pi\mu_p r/2}}{|\det(\mathbf{1} - \mathbf{J}_p^r)|^{1/2}}\right).$$

S_p denotes the classical action and μ_p is the Maslov index. As the group-theoretic factorizations that we shall develop here rely only on the linearity of evolution operators, they will apply to both the classical and the quantum cases.

For evaluation of spectra, the expansion (5) can be used pretty much as it stands[20], it can be expanded as a multinomial in cycle weights[47], or the leading eigenvalues can be extracted from the associated dynamical zeta function[5]

$$1/\zeta = \prod_p (1 - t_p), \quad t_p = z^{n_p}/\Lambda_p \quad \text{or} \quad t_p = e^{\frac{i}{\hbar} S_p(E) - i\pi\mu_p/2}/\Lambda_p^{1/2}, \quad (6)$$

obtained by approximating $\det(\mathbf{1} - \mathbf{J}_p) = \prod_{a=1}^d (1 - \Lambda_{p,a})$ by the product of expanding eigenvalues $\Lambda_p = |\prod_a \Lambda_{p,a}|$ in (5). For example, for a 1-dimensional expanding map each periodic point contributes with the weight $1/|1 - \Lambda_p^r|$:

$$\sum_{n=1}^{\infty} \frac{z^n}{n} \operatorname{tr} \mathcal{L}^n = \sum_p \sum_{r=1}^{\infty} \frac{1}{r} \frac{z^{n_p r}}{|1 - \Lambda_p^r|}.$$

Substituting $1/|1 - \Lambda| = |\Lambda|^{-1}(1 - \Lambda^{-1})^{-1} = |\Lambda|^{-1} \sum \Lambda^{-k}$ we obtain

$$\begin{aligned} \det(1 - z\mathcal{L}) &= \exp\left(-\sum_p \sum_{k=0}^{\infty} \sum_{r=1}^{\infty} \frac{1}{r} \left(\frac{z^{np}}{|\Lambda_p| \Lambda_p^k}\right)^r\right) \\ &= \prod_p \prod_{k=0}^{\infty} \left(1 - \frac{t_p}{\Lambda_p^k}\right), \quad t_p = \frac{z^{np}}{|\Lambda_p|}. \end{aligned} \quad (7)$$

The dynamical zeta function (6) is the $k = 0$ part of the above Selberg-type product. The full zeta functions (5) are infinite products over dynamical zeta functions which depend on both the expanding and the contracting eigenvalues. Most of the developments below are independent of the precise form of the zeta functions.

As the dynamical zeta functions have particularly simple cycle expansions, a simple geometrical shadowing interpretation of their convergence, and as they suffice for determination of leading eigenvalues, we shall concentrate in this paper on their factorizations; the full $Z(z)$ determinants can be factorized by the same techniques. To emphasize the group theoretic structure of zeta functions, we shall combine all the non-group-theory dependence of a p -cycle into a cycle weight t_p . We shall also often absorb z into the transfer operator: $z\mathcal{L} \rightarrow \mathcal{L}$, $z^{np}t_p \rightarrow t_p$.

The first prerequisite for converting expressions like (6) into cycle expansions is efficient enumeration of periodic orbits - the problem to which we turn next.

2.2 Symbolic dynamics

The key to a theory of a chaotic dynamical system is its qualitative, topological description[2], or, as it is usually called, its *symbolic dynamics*. The strategy is to partition phase space into topologically distinct regions, associate with each region a symbol from an *alphabet*, and use those symbols to label every possible trajectory. *Covering* symbolic dynamics assigns a distinct label to each distinct trajectory, though there might be symbol sequences which are not realized as trajectories. If all possible symbol sequences can be realized as physical trajectories, the symbolic dynamics is called *complete*; if some sequences are not allowed, the symbolic dynamics is *pruned* (the word is suggested by “pruning” of branches corresponding to forbidden sequences for symbolic dynamics organized hierarchically into a tree structure). In that case the alphabet must be supplemented by a *grammar*, a set of pruning rules. A periodic symbol string corresponds to a periodic orbit or a *cycle*. Periodic orbits will here be distinguished by a bar over the primitive symbol block,

but we often omit the bar if it is clear from the context that we are dealing with a periodic orbit.

These concepts are easily illustrated by the pinball models that we shall study here. Consider the motion of a point particle in a plane with N elastically reflecting convex disks. Any trajectory can be labelled by the sequence of disk bounces, and a symbolic dynamics is given by the alphabet of N symbols $\{1, 2, 3, \dots, N\}$. As the bodies are convex, there can be no two consecutive reflections off the same disk, hence the first rule of the grammar of allowed sequences is that symbol repetitions $_11_$, $_22_$, \dots , $_NN_$ are forbidden. More generally, we shall refer to a symbolic dynamics as an “ N -disk” symbolic dynamics if the phase space can be partitioned in N distinct regions such that an orbit starting in a partition can in one step reach all other partitions except itself.

A finite length scattering trajectory is not uniquely specified by its (finite) symbol sequence, but an unstable cycle (consisting of infinitely many repetitions of a prime building block) is. We shall show in sect. 3 that the prime cycles for such simple grammars are easily enumerated; for example, table 1 contains a list of all prime 3-disk cycles up to length 9, and table 2 contains a list of prime 4-disk cycles.

An important effect of a discrete symmetry is that it tessellates the phase space into copies of a fundamental domain, and thus induces a natural partition of phase space. The group elements $g = \{a, b, \dots, d\}$ which map the fundamental domain \tilde{M} into its copies $g\tilde{M}$, can double in function as letters of a symbolic dynamics alphabet. If the dynamics is symmetric under interchanges of disks, the absolute disk labels $\epsilon_i = 1, 2, \dots, N$ can be replaced by the symmetry-invariant relative disk→disk increments g_i , where g_i is the discrete group element that maps disk $i - 1$ into disk i . Experience shows that more often than not specifics of the model at hand dictate the choice of symmetry reduced symbolic dynamics, so rather than attempting to develop a general procedure here, we shall demonstrate the reduction for a series of specific examples in sect. 6. An immediate gain arising from symmetry invariant relabelling is that N -disk symbolic dynamics becomes $(N - 1)$ -nary, with no restrictions on the allowed sequences[40, 48]. However, the main gain is in the close connection between the symbol string symmetries and the phase space symmetries which will aid us in the zeta function factorizations. Once the connection between the full space and the reduced space is established, working in the fundamental domain (*ie.*, with irreducible segments) is so much simpler that we never use the full space orbits in actual computations.

Whether this symbolic dynamics is complete (as is the case for sufficiently separated disks), pruned (for example, for touching disks), or only a first coarse graining of the topology (as, for example, in systems with islands of stability) depends on the details of the dynamics and requires further case-by-case investigation. In the N -disk model outlined above we have tacitly assumed that the disks are sufficiently separated so that all possible symbol sequences (excluding symbol repeats) are realized as physical trajectories. If the disks shadow each other, further infinite families of sequences are pruned[49, 50, 51]. Determining the pruning rules is in general a highly non-trivial undertaking, carried out so far for only a few dynamical systems[7, 52]. In this paper we assume that the disks are sufficiently separated so that there is no additional pruning beyond self bounces. This assumption does not affect our main result, the symmetry induced factorizations – it only affects the cycle counting of sect. 3.

2.3 Cycle expansions

In the simplest of the cases that we shall discuss here (an example is the fundamental domain symmetric subspace of a 3-disk repeller, discussed in sect. 7.2) the system is described by a complete binary symbolic dynamics. The Euler product (6) is given by[18]

$$\begin{aligned}
1/\zeta = & (1 - zt_0)(1 - zt_1)(1 - z^2t_{01})(1 - z^3t_{001})(1 - z^3t_{011}) \\
& (1 - z^4t_{0001})(1 - z^4t_{0011})(1 - z^4t_{0111})(1 - z^5t_{00001})(1 - z^5t_{00011}) \\
& (1 - z^5t_{00101})(1 - z^5t_{00111})(1 - z^5t_{01011})(1 - z^5t_{01111}) \dots \quad (8)
\end{aligned}$$

The cycle expansion is obtained by multiplying out the Euler product and grouping together the terms of the same total string length (same power of z):

$$\begin{aligned}
1/\zeta = & 1 - zt_0 - zt_1 - z^2[(t_{01} - t_1t_0)] \\
& - z^3[(t_{001} - t_{01}t_0) - (t_{011} - t_{01}t_1)] \\
& - z^4[(t_{0001} - t_0t_{001}) + (t_{0111} - t_{011}t_1) \\
& + (t_{0011} - t_{001}t_1 - t_0t_{011} + t_0t_{01}t_1)] - \dots \quad (9)
\end{aligned}$$

The terms grouped in brackets are the *curvature* corrections[53]; the terms grouped in parenthesis are combinations of longer orbits and their shorter “shadowing” approximants. In the counting limit $t_p = 1$, and all such shadowing combinations vanish (as we show in more detail in sect. 3). The practical utility of

cycle expansions, in contrast to direct averages over periodic orbits such as in the trace formula[12], lies precisely in this organization into nearly cancelling combinations: cycle expansions are dominated by short cycles, with long cycles giving exponentially decaying corrections.

Further examples of cycle expansions are given in sect. 6 and in the Appendix.

3 Counting cycles

In this section we apply the cycle-counting methods of ref. [18] to the N -disk problem. This section is not essential to the main, group-theoretic thrust of this paper, but in practice cycle counting is of some use as a check of correctness of various cycle expansions.

There are $N_n = N^n$ possible distinct strings of length n composed of N letters. These N_n strings include all M_d prime cycles whose period d equals or divides n , and each d -cycle contributes its cyclic permutations, d in number:

$$N_n = \sum_{d|n} dM_d. \quad (10)$$

The number of prime cycles follows by Möbius inversion[54]

$$M_n = n^{-1} \sum_{d|n} \mu\left(\frac{n}{d}\right) N_d. \quad (11)$$

where $\mu(1) = 1$, $\mu(n) = 0$ if n has a squared factor, and $\mu(p_1 p_2 \dots p_k) = (-1)^k$ if all prime factors are different.

For example, from two symbols $\{0, 1\}$ one can form $M_n = 2, 1, 2, 3, 6, 9, 18, \dots$ prime cycles, *i.e.*, there are two fixed points $\overline{0}$ and $\overline{1}$, one prime 2-cycle $\overline{01}$, two 3-cycles $\overline{001}$ and $\overline{011}$, three 4-cycles $\overline{0001}$, $\overline{0011}$, $\overline{0111}$ (note that *e.g.* $\overline{1010} = \overline{01}^2$ is not prime), and so forth. In table 3 we list the number of prime orbits up to length 10 for 2-, 3- and 4-letter complete symbolic dynamics.

For a generic dynamical system not all M_n prime periodic symbol strings are realized as physical orbits: in such cases M_n is only an upper bound to the actual number of prime n -cycles. To count correctly, we need to *prune* the disallowed orbits, *ie.* specify the grammar of the allowed sequences. A simple example of pruning is the exclusion of “self-bounces” in the N -disk pinball. To determine the number of periodic orbits, consider a $[N \times N]$ transfer matrix whose elements are

$T_{ij} = 1$ if a transition from disk j to disk i is possible, and 0 otherwise. The number of points that are mapped back onto themselves after n iterations is given by $N_n = \text{tr } T^n$. For a complete N -ary dynamics all entries would equal unity

$$T_c = \begin{pmatrix} 1 & 1 & \dots & 1 \\ 1 & 1 & \dots & 1 \\ \vdots & \vdots & \ddots & \vdots \\ 1 & 1 & \dots & 1 \end{pmatrix}, \quad (12)$$

and $\text{tr } T_c^n = N^n$. The pruning of self-bounces eliminates the diagonal entries, $T_{N-disk} = T_c - \mathbf{1}$, so the number of the N -disk periodic points is

$$N_n = \text{tr } T_{N-disk}^n = (N-1)^n + (-1)^n(N-1). \quad (13)$$

Möbius inversion (11) now yields

$$\begin{aligned} M_n^{N-disk} &= \frac{1}{n} \sum_{d|n} \mu\left(\frac{n}{d}\right) (N-1)^d + \frac{N-1}{n} \sum_{d|n} \mu\left(\frac{n}{d}\right) (-1)^d \\ &= M_n^{(N-1)} \quad \text{for } n > 2. \end{aligned} \quad (14)$$

There are no fixed points, $M_1^{N-disk} = 0$. The number of periodic points of period 2 is $N^2 - N$, hence there are $M_2^{N-disk} = N(N-1)/2$ prime cycles of length 2; for lengths $n > 2$, the number of prime cycles is the same as for the complete $(N-1)$ -ary dynamics.

The simplest application of the cycle expansion of dynamical zeta function (6) is the evaluation of the *topological entropy*. The topological entropy is the growth rate of the number of orbits as a function of the length of their symbol sequences:

$$h = \lim_{n \rightarrow \infty} \ln N_n/n. \quad (15)$$

The topological entropy is given by the logarithm of the largest eigenvalue of the transition matrix T such as the one given in the above example. Dynamical zeta functions enter via the relationship (see eq. (18) of ref. [18])

$$\det(1 - zT) = \prod_p (1 - t_p), \quad (16)$$

where for the topological entropy the weight assigned to a prime cycle p of length n_p is $t_p = z^{n_p}$ if the cycle is allowed, or $t_p = 0$ if it is pruned. Expanded in powers of z one finds

$$\zeta(z)^{-1} = \prod_p (1 - t_p) = 1 + \sum_{k=1}^{\infty} z^k c_k. \quad (17)$$

This function is called the topological zeta function[2, 55]; if the grammar is finite, it reduces to the topological polynomial. The topological entropy h is given by the smallest zero $z = e^{-h}$.

For complete symbolic dynamics of N symbols, the topological polynomial is simply

$$\zeta(z)^{-1} = 1 - Nz, \quad (18)$$

whence the topological entropy $h = \ln N$.

One consequence of the finiteness of topological polynomials is that the contributions to curvatures at every order are even in number, half with positive and half with negative sign. For instance, for complete binary labelling (9),

$$\begin{aligned} c_4 = & -t_{0001} - t_{0011} - t_{0111} - t_0 t_{01} t_1 \\ & + t_0 t_{001} + t_0 t_{011} + t_{001} t_1 + t_{011} t_1. \end{aligned} \quad (19)$$

We see that 2^3 terms contribute to c_4 , and exactly half of them appear with a negative sign - hence if all binary strings are allowed, this term vanishes in the counting expression. The number of terms can be counted using the identity

$$\prod_p (1 + t_p) = \prod_p \frac{1 - t_p^2}{1 - t_p}. \quad (20)$$

Substituting (18) we obtain

$$\prod_p (1 + t_p) = \frac{1 - Nz^2}{1 - Nz} = 1 + Nz + \sum_{k=2}^{\infty} z^k (N^k - N^{k-1}). \quad (21)$$

The z^n coefficient in the above expansion is the number of terms contributing to c_n , so we find that for complete symbolic dynamics of N symbols and $n > 1$, the number of terms contributing to c_n is $(N - 1)N^{n-1}$.

This technique is easily generalized to cycle expansions for the N-disk symbol sequences. Consider for example the 3-disk pinball. The prohibition of repeating a symbol affects counting only for the fixed points and the 2-cycles. Everything else is the same as counting for a complete binary dynamics (eq (14)). To obtain the topological zeta function, just divide out the binary 1- and 2-cycles $(1 - zt_0)(1 - zt_1)(1 - z^2 t_{01})$ and multiply with the correct 3-disk 2-cycles $(1 - z^2 t_{12})(1 - z^2 t_{13})(1 - z^2 t_{23})$:

$$\begin{aligned} 1/\zeta_{3-disk} &= (1 - 2z) \frac{(1 - z^2)^3}{(1 - z)^2 (1 - z^2)} \\ &= (1 - 2z)(1 + z)^2 = 1 - 3z^2 - 2z^3. \end{aligned} \quad (22)$$

The 4-disk pinball topological polynomial can be derived in the same way: the pruning affects again only the fixed points and the 2-cycles

$$\begin{aligned} 1/\zeta_{4-disk} &= (1-3z) \frac{(1-z^2)^6}{(1-z)^3(1-z^2)^3} \\ &= (1-3z)(1+z)^3 = 1 - 6z^2 - 8z^3 - 3z^4, \end{aligned} \quad (23)$$

and, more generally, for an N -disk pinball, the topological polynomial is given by

$$\begin{aligned} 1/\zeta_{N-disk} &= (1-(N-1)z) \frac{(1-z^2)^{N(N-1)/2}}{(1-z)^{N-1}(1-z^2)^{(N-1)(N-2)/2}} \\ &= (1-(N-1)z)(1+z)^{N-1}. \end{aligned} \quad (24)$$

The topological polynomial has a root $z^{-1} = N - 1$, as we already know it should from (13). We shall see in sect. 6 that the other roots reflect the symmetry factorizations of zeta functions. Since the zeta functions reduce to polynomials, we are assured that there are just a few fundamental cycles and that all long cycles can be grouped into curvature combinations. For example, the fundamental cycles in (22) are the three 2-cycles which bounce back and forth between two disks and the two 3-cycles which visit every disk. It is only after these fundamental cycles have been included that a cycle expansion is expected to start converging smoothly, *i.e.*, only for n larger than the lengths of the fundamental cycles are the curvatures c_n , a measure of the deviations between long orbits and their short cycle approximants, expected to fall off rapidly with n .

Conversely, if the grammar is not finite and there is no finite topological polynomial, there will be no ‘‘curvature’’ expansions, and the convergence will be poor. That is the generic case, and one strategy[18, 51, 52] for dealing with it is to find a good sequence of approximate but finite grammars; for each approximate grammar cycle expansions yield exponentially accurate eigenvalues, with successive approximate grammars converging toward the desired infinite grammar system.

The N -disk topological zeta function may also be used to count the number of terms in the curvatures. For example, for the 3-disk pinball we get

$$\prod_p (1+t_p) = \frac{1-3z^4-2z^6}{1-3z^2-2z^3} = 1 + 3z^2 + 2z^3 + \frac{z^4(6+12z+2z^2)}{1-3z^2-2z^3} \quad (25)$$

The coefficients are 1, 0, 3, 2, 6, 12, 20, 48, 84, 184, \dots . That means that, *e.g.*, c_6 has a total of 20 terms, in agreement with the explicit 3-disk cycle expansion (62) of the appendix.

The above concludes our review of cycle expansions for general dynamical systems; now we turn to the main subject of this paper, the role of discrete symmetries in cycle expansions.

4 Discrete symmetries

A dynamical system is invariant under a symmetry group $G = \{e, g_2, \dots, g_g\}$ if the equations of motion are invariant under all symmetries $g \in G$. For a map $x_{n+1} = f(x_n)$ and the evolution operator $\mathcal{L}(y, x)$ defined by (2) this means

$$\begin{aligned} f(x) &= \mathbf{g}^{-1}f(\mathbf{g}x) \\ \mathcal{L}(y, x) &= \mathcal{L}(\mathbf{g}y, \mathbf{g}x) . \end{aligned} \tag{26}$$

Bold face letters for group elements indicate a suitable representation on phase space. For example, if a 2-dimensional map has the symmetry $x_1 \rightarrow -x_1, x_2 \rightarrow -x_2$, the symmetry group G consists of the identity and C , a rotation by π around the origin. The map f must then commute with rotations by π , $f(\mathbf{C}x) = \mathbf{C}f(x)$, with \mathbf{C} given by the $[2 \times 2]$ matrix

$$\mathbf{C} = \begin{bmatrix} -1 & 0 \\ 0 & -1 \end{bmatrix} . \tag{27}$$

C satisfies $C^2 = e$ and can be used to decompose the phase space into mutually orthogonal symmetric and antisymmetric subspaces by means of projection operators

$$\begin{aligned} P_{A_1} &= \frac{1}{2}(\mathbf{e} + \mathbf{C}) , & P_{A_2} &= \frac{1}{2}(\mathbf{e} - \mathbf{C}) , \\ \mathcal{L}_{A_1}(y, x) &= P_{A_1}\mathcal{L}(y, x) = \frac{1}{2}(\mathcal{L}(y, x) + \mathcal{L}(-y, x)) , \\ \mathcal{L}_{A_2}(y, x) &= P_{A_2}\mathcal{L}(y, x) = \frac{1}{2}(\mathcal{L}(y, x) - \mathcal{L}(-y, x)) . \end{aligned} \tag{28}$$

More generally[25, 26] the projection operator onto the α irreducible subspace of dimension d_α is given by $P_\alpha = (d_\alpha/|G|) \sum \chi_\alpha(h)\mathbf{h}^{-1}$, where $\chi_\alpha(h) = \text{tr } D_\alpha(h)$ are the group characters, and the transfer operator \mathcal{L} splits into a sum of inequivalent irreducible subspace contributions $\sum_\alpha \text{tr } \mathcal{L}_\alpha$,

$$\mathcal{L}_\alpha(y, x) = \frac{d_\alpha}{|G|} \sum_{h \in G} \chi_\alpha(h)\mathcal{L}(\mathbf{h}^{-1}y, x) . \tag{29}$$

The prefactor d_α in the above reflects the fact that a d_α -dimensional representation occurs d_α times.

4.1 Cycle degeneracies

If $g \in G$ is a symmetry of the dynamical problem, the weight of a cycle p and the weight of its image under a symmetry transformation g are equal, $t_{gp} = t_p$. The number of degenerate cycles (topologically distinct, but mapped into each other by symmetry transformations) depends on the cycle symmetries. Associated with a given cycle p is a maximal subgroup $\mathcal{H}_p \subseteq G$, $\mathcal{H}_p = \{e, b_2, b_3, \dots, b_h\}$ of order h_p , whose elements leave p invariant. The elements of the quotient space $b \in G/\mathcal{H}_p$ generate the degenerate cycles bp , so the multiplicity of a degenerate cycle is $m_p = g/h_p$.

Taking into account these degeneracies, the Euler product (6) takes the form

$$\prod_p (1 - t_p) = \prod_{\hat{p}} (1 - t_{\hat{p}})^{m_{\hat{p}}}. \quad (30)$$

Here \hat{p} is one of the m_p degenerate cycles, picked to serve as the label for the entire class. Our labelling convention is usually lexical, *i.e.*, we label a cycle p by the cycle point whose label has the lowest value, and we label a class of degenerate cycles by the one with the lowest label \hat{p} . In what follows we shall drop the hat in \hat{p} when it is clear from the context that we are dealing with symmetry distinct classes of cycles.

4.2 Example: C_{3v} invariance

An illustration of the above is afforded by C_{3v} , the group of symmetries of a pinball with three equal size, equally spaced disks, fig. 1. The group consists[56] of the identity element e , three reflections across axes $\{\sigma_{12}, \sigma_{23}, \sigma_{13}\}$, and two rotations by $2\pi/3$ and $4\pi/3$ denoted $\{C_3, C_3^2\}$, so its dimension is $g = 6$. On the disk labels $\{1, 2, 3\}$ these symmetries act as permutations which map cycles into cycles. For example, the flip across the symmetry axis going through disk 1 interchanges the symbols 2 and 3; it maps the cycle $\overline{12123}$ into $\overline{13132}$, fig. 2a.

The subgroups of C_{3v} are C_v , consisting of the identity and any one of the reflections, of dimension $h = 2$, and $C_3 = \{e, C_3, C_3^2\}$, of dimension $h = 3$, so possible cycle multiplicities are $g/h = 2, 3$ or 6 .

The C_3 subgroup invariance is exemplified by the cycles $\overline{123}$ and $\overline{132}$ which are invariant under rotations by $2\pi/3$ and $4\pi/3$, but are mapped into each other by any reflection, fig. 2b; $\mathcal{H}_p = \{e, C_3, C_3^2\}$, and the degeneracy is $g/h_{c_3} = 2$.

The C_v type of a subgroup is exemplified by the invariances of $\hat{p} = 1213$. This cycle is invariant under reflection $\sigma_{23}\{\overline{1213}\} = \overline{1312} = \overline{1213}$, so the invariant subgroup is $\mathcal{H}_{\hat{p}} = \{e, \sigma_{23}\}$. Its order is $h_{C_v} = 2$, so the degeneracy is $m_{\hat{p}} = g/h_{C_v} = 3$; the cycles in this class, $\overline{1213}$, $\overline{1232}$ and $\overline{1323}$, are related by $2\pi/3$ rotations, fig. 2c.

A cycle of no symmetry, such as $\overline{12123}$, has $\mathcal{H}_p = \{e\}$ and contributes in all six terms (the remaining cycles in the class are $\overline{12132}$, $\overline{12313}$, $\overline{12323}$, $\overline{13132}$ and $\overline{13232}$), fig. 2a.

Besides the above discrete symmetries, for Hamiltonian systems cycles may be related by time reversal symmetry. An example[57] are the cycles $\overline{121212313}$ and $\overline{121212323} = \overline{313212121}$ which are related by no space symmetry (fig. 2d).

The Euler product (6) for the C_{3v} symmetric 3-disk problem is given in the Appendix, eq. (62).

5 Dynamics in the fundamental domain

So far we have used the discrete symmetry to effect a reduction in the number of independent cycles in cycle expansions. The next step achieves much more: the symmetries can be used to restrict all computations to a *fundamental domain*. We show here that to each global cycle p corresponds a fundamental domain cycle \tilde{p} . Conversely, each fundamental domain cycle \tilde{p} traces out a segment of the global cycle p , with the end point of the cycle \tilde{p} mapped into the irreducible segment of p with the group element $h_{\tilde{p}}$.

If the dynamics is invariant under a discrete symmetry, the phase space M can be completely tiled by the fundamental domain \tilde{M} and its images $a\tilde{M}$, $b\tilde{M}$, ... under the action of the symmetry group $G = \{e, a, b, \dots\}$,

$$M = \sum_{a \in G} M_a = \sum_{a \in G} a\tilde{M}.$$

In the above example (27) with symmetry group $G = \{e, C\}$, the phase space $M = \{x_1-x_2 \text{ plane}\}$ can be tiled by a fundamental domain $\tilde{M} = \{\text{half-plane } x_1 \geq 0\}$, and $C\tilde{M} = \{\text{half-plane } x_1 \leq 0\}$, its image under rotation by π .

If the space M is decomposed into g tiles, a function $\phi(x)$ over M splits into a g -dimensional vector $\phi_a(x)$ defined by $\phi_a(x) = \phi(x)$ if $x \in M_a$, $\phi_a(x) = 0$ otherwise. Let $h = ab^{-1}$ be the symmetry operation that maps the endpoint domain M_b into the starting point domain M_a , and let $D(h)_{ba}$, the left regular representation, be

the $[g \times g]$ matrix whose b, a -th entry equals unity if $a = hb$ and zero otherwise; $D(h)_{ba} = \delta_{hb,a}$. Since the symmetries act on phase space as well, the operation h enters in two guises: as a $[g \times g]$ matrix $D(h)$ which simply permutes the domain labels, and as a $[d \times d]$ matrix representation \mathbf{h} of a discrete symmetry operation on the d phase-space coordinates. For instance, in the above example (27) $h \in C_2$ and $D(h)$ can be either the identity or the interchange of the two domain labels,

$$D(e) = \begin{bmatrix} 1 & 0 \\ 0 & 1 \end{bmatrix}, \quad D(C) = \begin{bmatrix} 0 & 1 \\ 1 & 0 \end{bmatrix}. \quad (31)$$

Note that $D(h)$ is a permutation matrix, mapping a tile M_a into a different tile $M_{ha} \neq M_a$ if $h \neq e$. Consequently only $D(e)$ has diagonal elements, and $\text{tr } D(h) = g\delta_{h,e}$. However, the phase-space transformation $\mathbf{h} \neq \mathbf{e}$ leaves invariant sets of *boundary* points; for example, under reflection σ across a symmetry axis, the axis itself remains invariant. The boundary periodic orbits that belong to such point-wise invariant sets will require special care in $\text{tr } \mathcal{L}$ evaluations.

One can associate to the evolution operator (2) a $[g \times g]$ matrix evolution operator defined by

$$\mathcal{L}_{ba}(y, x) = D(h)_{ba} \mathcal{L}(y, x),$$

if $x \in M_a$ and $y \in M_b$, and zero otherwise. Now we can use the invariance condition (26) to move the starting point x into the fundamental domain $x = \mathbf{a}\tilde{x}$, $\mathcal{L}(y, x) = \mathcal{L}(\mathbf{a}^{-1}y, \tilde{x})$, and then use the relation $a^{-1}b = h^{-1}$ to also relate the endpoint y to its image in the fundamental domain, $\tilde{\mathcal{L}}(\tilde{y}, \tilde{x}) \equiv \mathcal{L}(\mathbf{h}^{-1}\tilde{y}, \tilde{x})$. With this operator which is restricted to the fundamental domain, the global dynamics reduces to

$$\mathcal{L}_{ba}(y, x) = D(h)_{ba} \tilde{\mathcal{L}}(\tilde{y}, \tilde{x}).$$

While the global trajectory runs over the full space M , the restricted trajectory is brought back into the fundamental domain \tilde{M} any time it crosses into adjoining tiles; the two trajectories are related by the symmetry operation h which maps the global endpoint into its fundamental domain image.

Now the traces (4) required for the evaluation of the eigenvalues of the transfer operator can be evaluated on the fundamental domain alone

$$\text{tr } \mathcal{L} = \int_M dx \mathcal{L}(x, x) = \int_{\tilde{M}} d\tilde{x} \sum_h \text{tr } D(h) \mathcal{L}(\mathbf{h}^{-1}\tilde{x}, \tilde{x}) \quad (32)$$

The fundamental domain integral $\int d\tilde{x} \mathcal{L}(\mathbf{h}^{-1}\tilde{x}, \tilde{x})$ picks up a contribution from every global cycle (for which $h = e$), but it also picks up contributions from shorter segments of global cycles. The permutation matrix $D(h)$ guarantees by the identity $\text{tr} D(h) = 0$, $h \neq e$, that only those repeats of the fundamental domain cycles \tilde{p} that correspond to complete global cycles p contribute. Compare, for example, the contributions of the $\overline{12}$ and $\overline{0}$ cycles of fig. 3. $\text{tr} D(h)\tilde{\mathcal{L}}$ does not get a contribution from the $\overline{0}$ cycle, as the symmetry operation that maps the first half of the $\overline{12}$ into the fundamental domain is a reflection, and $\text{tr} D(\sigma) = 0$. In contrast, $\sigma^2 = e$, $\text{tr} D(\sigma^2) = 6$ insures that the repeat of the fundamental domain fixed point $\text{tr} (D(h)\tilde{\mathcal{L}})^2 = 6t_0^2$, gives the correct contribution to the global trace $\text{tr} \mathcal{L}^2 = 3 \cdot 2t_{12}$.

Let p be the full orbit, \tilde{p} the orbit in the fundamental domain and $h_{\tilde{p}}$ an element of \mathcal{H}_p , the symmetry group of p . Restricting the volume integrations to the infinitesimal neighborhoods of the cycles p and \tilde{p} , respectively, and performing the standard resummations[18], we obtain the identity

$$(1 - t_p)^{m_p} = \det(1 - D(h_{\tilde{p}})t_{\tilde{p}}) \ , \quad (33)$$

valid cycle by cycle in the Euler products (6) for $\det(1 - \mathcal{L})$. Here “det” refers to the $[g \times g]$ matrix representation $D(h_{\tilde{p}})$; as we shall see, this determinant can be evaluated in terms of standard characters, and no explicit representation of $D(h_{\tilde{p}})$ is needed. Finally, if a cycle p is invariant under the symmetry subgroup $\mathcal{H}_p \subseteq G$ of order h_p , its weight can be written as a repetition of a fundamental domain cycle

$$t_p = t_{\tilde{p}}^{h_p} \quad (34)$$

computed on the irreducible segment that corresponds to a fundamental domain cycle. For example, in fig. 3 we see by inspection that $t_{12} = t_0^2$ and $t_{123} = t_1^3$.

We conclude this section with a few comments about the role of symmetries in actual extraction of cycles. In the example at hand, the N -disk billiard systems, a fundamental domain is a sliver of the N -disk configuration space delineated by a pair of adjoining symmetry axes, with the directions of the momenta indicated by arrows. The flow may further be reduced to a return map on a Poincaré surface of section, on which an appropriate transfer operator may be constructed. While in principle any Poincaré surface of section will do, a natural choice in the present context are crossings of symmetry axes.

In actual numerical integrations only the last crossing of a symmetry line needs to be determined (using for example the method of ref. [58]). The cycle is run in

global coordinates and the group elements associated with the crossings of symmetry lines are recorded; integration is terminated when the orbit closes in the fundamental domain. Periodic orbits with non-trivial symmetry subgroups are particularly easy to find since their points lie on crossings of symmetry lines[59, 34]. A multi-point-shooting method combined with Newton-Raphson iteration has proven very efficient[50] in practice.

5.1 Boundary orbits

Before we can turn to a presentation of the factorizations of zeta functions for the different symmetries we have to discuss a peculiar effect that arises for orbits that run on a symmetry line that borders a fundamental domain[60, 26, 27]. In our 3-disk example, no such orbits are possible, but they exist in other systems, such as in the bounded region of the Hénon-Heiles potential and in 1-d maps. For the symmetrical 4-disk billiard, there are in principle two kinds of such orbits, one kind bouncing back and forth between two diagonally opposed disks and the other kind moving along the other axis of reflection symmetry; the latter exists for bounded systems only. While there are typically very few boundary orbits, they tend to be among the shortest orbits, and their neglect can seriously degrade the convergence of cycle expansions, as those are dominated by the shortest cycles.

While such orbits are invariant under some symmetry operations, their neighborhoods are not. This affects the stability matrix \mathbf{J}_p of the linearization perpendicular to the orbit and thus the eigenvalues. Typically, *e.g.* if the symmetry is a reflection, some eigenvalues of \mathbf{J}_p change sign. This means that instead of a weight $1/\det(\mathbf{1} - \mathbf{J}_p)$ as for a regular orbit, boundary cycles also pick up contributions of form $1/\det(\mathbf{1} - \mathbf{h}\mathbf{J}_p)$, where \mathbf{h} is a symmetry operation that leaves the orbit pointwise invariant; see for example sect. 6.3.

Consequences for the zeta function factorizations are that sometimes a boundary orbit does not contribute. A derivation of a dynamical zeta function (6) from a determinant like (5) usually starts with an expansion of the determinants of the Jacobian. The leading order terms just contain the product of the expanding eigenvalues and lead to the zeta function (6). Next to leading order terms contain products of expanding and contracting eigenvalues and are sensitive to their signs. Clearly, the weights t_p in the zeta functions will then be affected by reflections in the Poincaré surface of section perpendicular to the orbit. In all our applications it

was possible to implement these effects by the following simple prescription.

If an orbit is invariant under a little group $\mathcal{H}_p = \{e, b_2, \dots, b_n\}$, then the corresponding group element in (33) will be replaced by a projector. If the weights are insensitive to the signs of the eigenvalues, then this projector is

$$g_p = \frac{1}{h} \sum_{i=1}^h b_i. \quad (35)$$

In the cases that we have considered, the change of sign may be taken into account by defining a sign function $\epsilon_p(g) = \pm 1$, with the “-” sign if the symmetry element g flips the neighborhood. Then (35) is replaced by

$$g_p = \frac{1}{h} \sum_{i=1}^h \epsilon(b_i) b_i. \quad (36)$$

The resulting zeta functions agree with the ones given by Lauritzen[26]. We illustrate the above in sect. 6.3 by working out the full factorization for the 1-dimensional reflection symmetric maps.

6 Factorizations of zeta functions

In the above we have shown that a discrete symmetry induces degeneracies among periodic orbits and decomposes periodic orbits into repetitions of irreducible segments; this reduction to a fundamental domain furthermore leads to a convenient symbolic dynamics compatible with the symmetry, and, most importantly, to a factorization of zeta functions. This we now develop, first in a general setting and then for specific examples.

6.1 Factorizations of dynamical zeta functions

According to (33) and (34), the contribution of a degenerate class of global cycles (cycle p with multiplicity $m_p = g/h_p$) to a zeta function is given by the corresponding fundamental domain cycle \tilde{p} :

$$(1 - t_{\tilde{p}}^{h_p})^{g/h_p} = \det(1 - D(h_{\tilde{p}})t_{\tilde{p}}) \quad (37)$$

Let $D(h) = \bigoplus_{\alpha} d_{\alpha} D_{\alpha}(h)$ be the decomposition of the matrix representation $D(h)$ into the d_{α} dimensional irreducible representations α of a finite group G . Such

decompositions are block-diagonal, so the corresponding contribution to the Euler product (5) factorizes as

$$\det(1 - D(h)t) = \prod_{\alpha} \det(1 - D_{\alpha}(h)t)^{d_{\alpha}} , \quad (38)$$

where now the product extends over all distinct d_{α} -dimensional irreducible representations, each contributing d_{α} times. For the cycle expansion purposes, it has been convenient to emphasize that the group-theoretic factorization can be effected cycle by cycle, as in (37); but from the transfer operator point of view, the key observation is that the symmetry reduces the transfer operator to a block diagonal form; this block diagonalization implies that the zeta functions (6) factorize as

$$\frac{1}{\zeta} = \prod_{\alpha} \frac{1}{\zeta_{\alpha}^{d_{\alpha}}} , \quad \frac{1}{\zeta_{\alpha}} = \prod_{\bar{p}} \det(1 - D_{\alpha}(h_{\bar{p}})t_{\bar{p}}) . \quad (39)$$

Determinants of d -dimensional irreducible representations can be evaluated using the expansion of determinants in terms of traces,

$$\begin{aligned} \det(1 + M) &= 1 + \operatorname{tr} M + \frac{1}{2} \left((\operatorname{tr} M)^2 - \operatorname{tr} M^2 \right) \\ &\quad + \frac{1}{6} \left((\operatorname{tr} M)^3 - 3 (\operatorname{tr} M)(\operatorname{tr} M^2) + 2 \operatorname{tr} M^3 \right) \\ &\quad + \cdots + \frac{1}{d!} \left((\operatorname{tr} M)^d - \cdots \right) , \end{aligned} \quad (40)$$

and each factor in (38) can be evaluated by looking up the characters $\chi_{\alpha}(h) = \operatorname{tr} D_{\alpha}(h)$ in standard tables[56]. In terms of characters, we have for the 1-dimensional representations

$$\det(1 - D_{\alpha}(h)t) = 1 - \chi_{\alpha}(h)t ,$$

for the 2-dimensional representations

$$\det(1 - D_{\alpha}(h)t) = 1 - \chi_{\alpha}(h)t + \frac{1}{2} \left(\chi_{\alpha}(h)^2 - \chi_{\alpha}(h^2) \right) t^2 ,$$

and so forth. These expressions can sometimes be simplified further using standard group-theoretical methods. For example, the $\frac{1}{2}((\operatorname{tr} M)^2 - \operatorname{tr} M^2)$ term in (40) is the trace of the antisymmetric part of the $M \times M$ Kronecker product; if α is a 2-dimensional representation, this is the A_2 antisymmetric representation, so

$$\text{2-dim: } \det(1 - D_{\alpha}(h)t) = 1 - \chi_{\alpha}(h)t + \chi_{A_2}(h)t^2 . \quad (41)$$

In the fully symmetric subspace $\operatorname{tr} D_{A_1}(h) = 1$ for all orbits; hence a straightforward fundamental domain computation (with no group theory weights) always yields a part of the full spectrum. In practice this is the most interesting subspectrum, as it contains the leading eigenvalue of the transfer operator.

6.2 Factorizations of functional determinants

Factorization of the full functional determinant (4) proceeds in essentially the same manner as the factorization of dynamical zeta functions outlined above. By (29) and (32) the trace of the transfer operator \mathcal{L} splits into the sum of inequivalent irreducible subspace contributions $\sum_{\alpha} \text{tr } \mathcal{L}_{\alpha}$, with

$$\text{tr } \mathcal{L}_{\alpha} = d_{\alpha} \sum_{h \in G} \chi_{\alpha}(h) \int_{\tilde{M}} d\tilde{x} \mathcal{L}(\mathbf{h}^{-1}\tilde{x}, \tilde{x}).$$

This leads by standard manipulations[18, 46] to the factorization of (5) into

$$Z(z) = \prod_{\alpha} Z_{\alpha}(z)^{d_{\alpha}}, \quad Z_{\alpha}(z) = \exp \left(- \sum_{\tilde{p}} \sum_{r=1}^{\infty} \frac{1}{r} \frac{\chi_{\alpha}(h_{\tilde{p}}^r) z^{n_{\tilde{p}} r}}{|\det(\mathbf{1} - \tilde{\mathbf{J}}_{\tilde{p}}^r)|} \right), \quad (42)$$

where $\tilde{\mathbf{J}}_{\tilde{p}} = \mathbf{h}_{\tilde{p}} \mathbf{J}_{\tilde{p}}$ is the fundamental domain Jacobian. Boundary orbits require special treatment, discussed in sect. 5.1, with examples given in the next section as well as in sect. 7.

The factorizations (39), (42) are the main result of this paper. We now proceed to exemplify it by a few cases of physical interest. Additional examples (factorization and cycle expansions for the cyclic symmetry groups C_3 and C_N) are given in ref. [22].

6.3 Reflection symmetric 1-d maps: C_2 factorization

Consider f , a map on the interval with reflection symmetry $f(-x) = -f(x)$. Denote the reflection operation by $\mathbf{C}x = -x$. The symmetry of the map implies that if $\{x_n\}$ is a trajectory, than also $\{\mathbf{C}x_n\}$ is a trajectory because $\mathbf{C}x_{n+1} = \mathbf{C}f(x_n) = f(\mathbf{C}x_n)$. The dynamics can be restricted to a fundamental domain, in this case to one half of the original interval; every time a trajectory leaves this interval, it can be mapped back using \mathbf{C} .

To compute the traces of the symmetrization and antisymmetrization projection operators (28), we have to distinguish three kinds of cycles[61]: asymmetric cycles a , symmetric cycles s built by repeats of irreducible segments \tilde{s} , and boundary cycles b . The Fredholm determinant can be formally written as the product over the three kinds of cycles: $\det(1 - \mathcal{L}) = \det(1 - \mathcal{L})_a \det(1 - \mathcal{L})_{\tilde{s}} \det(1 - \mathcal{L})_b$.

Asymmetric cycles: A periodic orbits is not symmetric if $\{x_a\} \cap \{\mathbf{C}x_a\} = \emptyset$, where $\{x_a\}$ is the set of periodic points belonging to the cycle a . Thus \mathbf{C} generates a second orbit with the same number of points and the same stability properties. Both orbits give the same contribution to the first term and no contribution to the second term in (28); as they are degenerate, the prefactor 1/2 cancels. Resumming as in the derivation of (7), we find that asymmetric orbits yield the same contribution to the symmetric and the antisymmetric subspaces:

$$\det(1 - \mathcal{L}_\pm)_a = \prod_a \prod_{k=0}^{\infty} \left(1 - \frac{t_a}{\Lambda_a^k}\right), \quad t_a = \frac{z^{n_a}}{|\Lambda_a|}.$$

Symmetric cycles: A cycle s is reflection symmetric if operating with \mathbf{C} on the set of cycle points reproduces the set. The period of a symmetric cycle is always even ($n_s = 2n_{\tilde{s}}$) and the mirror image of the x_s cycle point is reached by traversing the irreducible segment \tilde{s} of length $n_{\tilde{s}}$, $f^{n_{\tilde{s}}}(x_s) = \mathbf{C}x_s$. $\delta(x - f^n(x))$ picks up $2n_{\tilde{s}}$ contributions for every even traversal, $n = rn_{\tilde{s}}$, r even, and $\delta(x + f^n(x))$ for every odd traversal, $n = rn_{\tilde{s}}$, r odd. Absorb the group-theoretic prefactor in the stability eigenvalue by defining $\Lambda_{\tilde{s}} = -Df^{n_{\tilde{s}}}(x_s)$, where $Df^{n_{\tilde{s}}}(x_s)$ is the stability computed for a segment of length $n_{\tilde{s}}$. Restricting the integration to the infinitesimal neighborhood of the s cycle, we obtain the contribution to $tr\mathcal{L}_\pm^n$:

$$\begin{aligned} z^n tr \mathcal{L}_\pm^n &\rightarrow \int_{V_s} dx z^n \frac{1}{2} (\delta(x - f^n(x)) \pm \delta(x + f^n(x))) \\ &= n_{\tilde{s}} \left(\sum_{r=2}^{\text{even}} \delta_{n, rn_{\tilde{s}}} \frac{t_{\tilde{s}}^r}{1 - 1/\Lambda_{\tilde{s}}^r} \pm \sum_{r=1}^{\text{odd}} \delta_{n, rn_{\tilde{s}}} \frac{t_{\tilde{s}}^r}{1 - 1/\Lambda_{\tilde{s}}^r} \right) \\ &= n_{\tilde{s}} \sum_{r=1}^{\infty} \delta_{n, rn_{\tilde{s}}} \frac{(\pm t_{\tilde{s}})^r}{1 - 1/\Lambda_{\tilde{s}}^r}. \end{aligned}$$

Substituting all symmetric cycles s into $\det(1 - \mathcal{L}_\pm)$ and resumming as in (7), we obtain:

$$\det(1 - \mathcal{L}_\pm)_{\tilde{s}} = \prod_{\tilde{s}} \prod_{k=0}^{\infty} \left(1 \mp \frac{t_{\tilde{s}}}{\Lambda_{\tilde{s}}^k}\right)$$

Boundary cycles: In the example at hand there is only one cycle which is neither symmetric nor antisymmetric, but lies on the boundary of the fundamental domain, the fixed point at the origin. Such a cycle contributes simultaneously to both

$\delta(x - f^n(x))$ and $\delta(x + f^n(x))$:

$$\begin{aligned}
z^n \text{tr } \mathcal{L}_\pm^n &\rightarrow \int_{V_b} dx z^n \frac{1}{2} (\delta(x - f^n(x)) \pm \delta(x + f^n(x))) \\
&= \sum_{r=1}^{\infty} \delta_{n,r} t_b^r \frac{1}{2} \left(\frac{1}{1 - 1/\Lambda_b^r} \pm \frac{1}{1 + 1/\Lambda_b^r} \right) \\
z^n \text{tr } \mathcal{L}_+^n &\rightarrow \sum_{r=1}^{\infty} \delta_{n,r} \frac{t_b^r}{1 - 1/\Lambda_b^{2r}}; \quad z^n \text{tr } \mathcal{L}_-^n \rightarrow \sum_{r=1}^{\infty} \delta_{n,r} \frac{1}{\Lambda_b^r} \frac{t_b^r}{1 - 1/\Lambda_b^{2r}}.
\end{aligned}$$

Boundary orbit contributions to the factorized Fredholm determinants follow by resummation:

$$\det(1 - \mathcal{L}_+)_b = \prod_{k=0}^{\infty} \left(1 - \frac{t_b}{\Lambda_b^{2k}} \right), \quad \det(1 - \mathcal{L}_-)_b = \prod_{k=0}^{\infty} \left(1 - \frac{t_b}{\Lambda_b^{2k+1}} \right)$$

Only even derivatives contribute to the symmetric subspace (and odd to the anti-symmetric subspace) because the orbit lies on the boundary. The symmetry reduced Fredholm determinants follows by collecting the above results:

$$\begin{aligned}
Z_+(z) &= \prod_a \prod_{k=0}^{\infty} \left(1 - \frac{t_a}{\Lambda_a^k} \right) \prod_{\tilde{s}} \prod_{k=0}^{\infty} \left(1 - \frac{t_{\tilde{s}}}{\Lambda_{\tilde{s}}^k} \right) \prod_{k=0}^{\infty} \left(1 - \frac{t_b}{\Lambda_b^{2k}} \right) \\
Z_-(z) &= \prod_a \prod_{k=0}^{\infty} \left(1 - \frac{t_a}{\Lambda_a^k} \right) \prod_{\tilde{s}} \prod_{k=0}^{\infty} \left(1 + \frac{t_{\tilde{s}}}{\Lambda_{\tilde{s}}^k} \right) \prod_{k=0}^{\infty} \left(1 - \frac{t_b}{\Lambda_b^{2k+1}} \right)
\end{aligned} \tag{43}$$

As reflection symmetry is essentially the only discrete symmetry that a map of the interval can have, this example completes the group-theoretic factorization of determinants and zeta functions for 1-dimensional maps. A specific example is worked out in Ref. [61]

7 Examples of symmetry induced factorizations

We conclude with several explicit examples of group theory factorizations of cycle expansions of dynamical zeta functions. These expansions are a prerequisite for applications of periodic orbit theory to the evaluation of classical and quantal spectra; in particular, they were used in the calculations of refs. [9, 42].

7.1 C_2 factorizations

As the simplest example of implementing the above scheme consider the C_2 symmetry which arises, for example, in the Lorenz system[29], in the 3-dimensional anisotropic Kepler problem[24, 30, 31] or in the cycle expansions treatments of the Ising model[62]. For our purposes, all that we need to know here is that each orbit or configuration is uniquely labelled by an infinite string $\{s_i\}$, $s_i = +, -$ and that the dynamics is invariant under the $+ \leftrightarrow -$ interchange, *i.e.*, it is C_2 symmetric. In the Lorenz system, the labels $+$ and $-$ stand for the left or the right lobe of the attractor and the symmetry is a rotation by π around the z-axis. Similarly, the Ising Hamiltonian (in the absence of an external magnetic field) is invariant under spin flip. The C_2 symmetry cycles separate into two classes, the self-dual configurations $+-, ++--, +++---, +--+-+ +- , \dots$, with multiplicity $m_p = 1$, and the asymmetric configurations $+, -, ++-, --+, \dots$, with multiplicity $m_p = 2$. For example, as there is no absolute distinction between the “up” and the “down” spins, or the “left” or the “right” lobe, $t_+ = t_-$, $t_{++-} = t_{+--}$, and so on.

The symmetry reduced labelling $\rho_i \in \{0, 1\}$ is related to the standard $s_i \in \{+, -\}$ Ising spin labelling by

$$\begin{aligned} \text{If } s_i &= s_{i-1} \text{ then } \rho_i = 1 \\ \text{If } s_i &\neq s_{i-1} \text{ then } \rho_i = 0 \end{aligned} \tag{44}$$

For example, $\overline{+} = \dots + + + + \dots$ maps into $\dots 111 \dots = \overline{1}$ (and so does $\overline{-}$), $\overline{+-} = \dots - + - + \dots$ maps into $\dots 000 \dots = \overline{0}$, $\overline{++-} = \dots - - + + - - + + \dots$ maps into $\dots 0101 \dots = \overline{01}$, and so forth. A list of such reductions is given in table 4.

Depending on the maximal symmetry group \mathcal{H}_p that leaves an orbit p invariant (*cf.* sects. 4, 5), the contributions to the zeta function factor as

$$\begin{aligned} & A_1 \quad A_2 \\ \mathcal{H}_p = \{e\} : & (1 - t_{\overline{p}})^2 = (1 - t_{\overline{p}})(1 - t_{\overline{p}}) \\ \mathcal{H}_p = \{e, \sigma\} : & (1 - t_{\overline{p}}^2) = (1 - t_{\overline{p}})(1 + t_{\overline{p}}), \end{aligned} \tag{45}$$

For example:

$$\begin{aligned} \mathcal{H}_{++-} = \{e\} : & (1 - t_{++-})^2 = (1 - t_{001})(1 - t_{001}) \\ \mathcal{H}_{+-} = \{e, \sigma\} : & (1 - t_{+-}) = (1 - t_0)(1 + t_0), \quad t_{+-} = t_0^2 \end{aligned}$$

This yields two binary expansions. The A_1 subspace zeta function is given by the standard binary expansion (9). The antisymmetric A_2 subspace zeta function ζ_{A_2} differs from ζ_{A_1} only by a minus sign for cycles with an odd number of 0's:

$$\begin{aligned}
1/\zeta_{A_2} &= (1+t_0)(1-t_1)(1+t_{10})(1-t_{100})(1+t_{101})(1+t_{1000}) \\
&\quad (1-t_{1001})(1+t_{1011})(1-t_{10000})(1+t_{10001}) \\
&\quad (1+t_{10010})(1-t_{10011})(1-t_{10101})(1+t_{10111}) \dots \\
&= 1+t_0-t_1+(t_{10}-t_1t_0)-(t_{100}-t_{10}t_0)+(t_{101}-t_{10}t_1) \\
&\quad -(t_{1001}-t_1t_{001}-t_{101}t_0+t_{10}t_0t_1)-\dots\dots\dots
\end{aligned} \tag{46}$$

Note that the group theory factors do not destroy the curvature corrections (the cycles and pseudo cycles are still arranged into shadowing combinations).

If the system under consideration has a boundary orbit (*cf.* sect. 5.1) with group-theoretic factor $\mathbf{h}_p = (\mathbf{e} + \sigma)/2$, the boundary orbit does not contribute to the antisymmetric subspace

$$\begin{array}{cc}
A_1 & A_2 \\
\text{boundary: } (1-t_p) &= (1-t_{\bar{p}})(1-0t_{\bar{p}})
\end{array} \tag{47}$$

This is the $1/\zeta$ part of the boundary orbit factorization of sect. 6.3.

7.2 3-disc pinball: C_{3v} factorization

The next example, the C_{3v} symmetry, can be worked out by a glance at fig. 3a. For the symmetric 3-disk pinball the fundamental domain is bounded by a disk segment and the two adjacent sections of the symmetry axes that act as mirrors (see fig. 3b). The three symmetry axes divide the space into six copies of the fundamental domain. Any trajectory on the full space can be pieced together from bounces in the fundamental domain, with symmetry axes replaced by flat mirror reflections. The binary $\{0, 1\}$ reduction of the ternary three disk $\{1, 2, 3\}$ labels has a simple geometric interpretation: a collision of type 0 reflects the projectile to the disk it comes from (back-scatter), whereas after a collision of type 1 projectile continues to the third disk. For example, $\overline{23} = \dots 232323 \dots$ maps into $\dots 000 \dots = \overline{0}$ (and so do $\overline{12}$ and $\overline{13}$), $\overline{123} = \dots 12312 \dots$ maps into $\dots 111 \dots = \overline{1}$ (and so does $\overline{132}$), and so forth. A list of such reductions for short cycles is given in table 5.

C_{3v} has two one-dimensional irreducible representations, symmetric and anti-symmetric under reflections, denoted A_1 and A_2 , and a pair of degenerate two-dimensional representations of mixed symmetry, denoted E . The contribution of an orbit with symmetry g to the $1/\zeta$ Euler product (38) factorizes according to

$$\det(1 - D(h)t) = (1 - \chi_{A_1}(h)t)(1 - \chi_{A_2}(h)t) \left(1 - \chi_E(h)t + \chi_{A_2}(h)t^2\right)^2 \quad (48)$$

with the three factors contributing to the C_{3v} irreducible representations A_1 , A_2 and E , respectively, and the 3-disk zeta function factorizes into $\zeta = \zeta_{A_1}\zeta_{A_2}\zeta_E^2$. Substituting the C_{3v} characters[56]

C_{3v}	A_1	A_2	E
e	1	1	2
C_3, C_3^2	1	1	-1
σ_v	1	-1	0

into (48), we obtain for the three classes of possible orbit symmetries (indicated in the first column)

$$\begin{array}{rcl}
\mathbf{h}_{\bar{p}} & & A_1 \quad A_2 \quad E \\
e : & (1 - t_{\bar{p}})^6 = & (1 - t_{\bar{p}})(1 - t_{\bar{p}})(1 - 2t_{\bar{p}} + t_{\bar{p}}^2)^2 \\
C_3, C_3^2 : & (1 - t_{\bar{p}}^3)^2 = & (1 - t_{\bar{p}})(1 - t_{\bar{p}})(1 + t_{\bar{p}} + t_{\bar{p}}^2)^2 \\
\sigma_v : & (1 - t_{\bar{p}}^2)^3 = & (1 - t_{\bar{p}})(1 + t_{\bar{p}})(1 + 0t_{\bar{p}} - t_{\bar{p}}^2)^2.
\end{array} \quad (49)$$

where σ_v stands for any one of the three reflections.

The Euler product (6) on each irreducible subspace follows from the factorization (49). On the symmetric A_1 subspace the ζ_{A_1} is given by the standard binary curvature expansion (8). The antisymmetric A_2 subspace ζ_{A_2} differs from ζ_{A_1} only by a minus sign for cycles with an odd number of 0's, and is given in (46). For the mixed-symmetry subspace E the curvature expansion is given by

$$\begin{aligned}
1/\zeta_E &= (1 + zt_1 + z^2t_1^2)(1 - z^2t_0^2)(1 + z^3t_{100} + z^6t_{100}^2)(1 - z^4t_{10}^2) \\
&\quad (1 + z^4t_{1001} + z^8t_{1001}^2)(1 + z^5t_{10000} + z^{10}t_{10000}^2) \\
&\quad (1 + z^5t_{10101} + z^{10}t_{10101}^2)(1 - z^5t_{10011})^2 \dots \\
&= 1 + zt_1 + z^2(t_1^2 - t_0^2) + z^3(t_{001} - t_1t_0^2) \\
&\quad + z^4 \left[t_{0011} + (t_{001} - t_1t_0^2)t_1 - t_{01}^2 \right] \\
&\quad + z^5 \left[t_{00001} + t_{01011} - 2t_{00111} + (t_{0011} - t_{01}^2)t_1 + (t_1^2 - t_0^2)t_{100} \right] + \dots \quad (50)
\end{aligned}$$

We have reinserted the powers of z in order to group together cycles and pseudocycles of the same length. Note that the factorized cycle expansions retain the curvature form; long cycles are still shadowed by (somewhat less obvious) combinations of pseudocycles.

Referring back to the topological polynomial (22) obtained by setting $t_p = 1$, we see that its factorization is a consequence of the C_{3v} factorization of the ζ function:

$$1/\zeta_{A_1} = 1 - 2z, \quad 1/\zeta_{A_2} = 1, \quad 1/\zeta_E = 1 + z,$$

as obtained from (8), (46) and (50) for $t_p = 1$.

An example of a system with C_{3v} symmetry is provided by the motion of a particle in the Hénon-Heiles potential[32]

$$V(r, \theta) = \frac{1}{2}r^2 + \frac{1}{3}r^3 \sin(3\theta).$$

Our coding is not directly applicable to this system because of the existence of elliptic islands and because the three orbits that run along the symmetry axis cannot be labelled in our code. However, since these orbits run along the boundary of the fundamental domain, they require the special treatment[26] discussed in sect. 5.1.

Their symmetry is $K = \{\mathbf{e}, \sigma\}$, so according to (35), they pick up the group-theoretic factor $\mathbf{h}_p = (\mathbf{e} + \sigma)/2$. If there is no sign change in t_p , then evaluation of $\det(1 - \frac{\mathbf{e} + \sigma}{2} t_{\bar{p}})$ yields

$$\begin{array}{ccc} A_1 & A_2 & E \\ \text{boundary: } (1 - t_p)^3 & = & (1 - t_{\bar{p}})(1 - 0t_{\bar{p}})(1 - t_{\bar{p}})^2, \quad t_p = t_{\bar{p}}. \end{array} \quad (51)$$

However, if the cycle weight changes sign under reflection, $t_{\sigma\bar{p}} = -t_{\bar{p}}$, the boundary orbit does not contribute to the subspace symmetric under reflection across the orbit;

$$\begin{array}{ccc} A_1 & A_2 & E \\ \text{boundary: } (1 - t_p)^3 & = & (1 - 0t_{\bar{p}})(1 - t_{\bar{p}})(1 - t_{\bar{p}})^2, \quad t_p = t_{\bar{p}}. \end{array} \quad (52)$$

7.3 C_{4v} factorization

If an N -disk arrangement has C_N symmetry, and the disk visitation sequence is given by disk labels $\{\epsilon_1\epsilon_2\epsilon_3\dots\}$, only the relative increments $\rho_i = \epsilon_{i+1} - \epsilon_i \bmod N$ matter. Symmetries under reflections across axes increase the group to C_{Nv} and

add relations between symbols: $\{\epsilon_i\}$ and $\{N - \epsilon_i\}$ differ only by a reflection[40, 48]. As a consequence of this reflection increments become decrements until the next reflection and vice versa. Consider four equal disks placed on the vertices of a square (fig.4). The symmetry group consists of the identity \mathbf{e} , the two reflections σ_x, σ_y across x, y axes, the two diagonal reflections σ_{13}, σ_{24} , and the three rotations C_4, C_2 and C_4^3 by angles $\pi/2, \pi$ and $3\pi/2$. We start by exploiting the C_4 subgroup symmetry in order to replace the absolute labels $\epsilon_i \in \{1, 2, 3, 4\}$ by relative increments $\rho_i \in \{1, 2, 3\}$. By reflection across diagonals, an increment by 3 is equivalent to an increment by 1 and a reflection; this new symbol will be called $\underline{1}$. Our convention will be to first perform the increment and then to change the orientation due to the reflection. As an example, consider the fundamental domain cycle 112. Taking the disk 1 \rightarrow disk 2 segment as the starting segment, this symbol string is mapped into the disk visitation sequence $1_{+1}2_{+1}3_{+2}1 \dots = \overline{123}$, where the subscript indicates the increments (or decrements) between neighboring symbols; the period of the cycle $\overline{112}$ is thus 3 in both the fundamental domain and the full space. Similarly, the cycle $\underline{112}$ will be mapped into $1_{+1}2_{-1}1_{-2}3_{-1}2_{+1}3_{+2}1 = \overline{121323}$ (note that the fundamental domain symbol $\underline{1}$ corresponds to a flip in orientation after the second and fifth symbols); this time the period in the full space is twice that of the fundamental domain. In particular, the fundamental domain fixed points correspond to the following 4-disk cycles:

4-disk		reduced
12	\leftrightarrow	$\underline{1}$
1234	\leftrightarrow	1
13	\leftrightarrow	2

Conversions for all periodic orbits of reduced symbol period less than 5 are listed in table 6.

While there is a variety of labelling conventions[57, 48, 39] for the reduced C_{4v} dynamics, we prefer the one introduced here because of its close relation to the group-theoretic structure of the dynamics: the global 4-disk trajectory can be generated by mapping the fundamental domain trajectories onto the full 4-disk space by the accumulated product of the C_{4v} group elements $g_1 = C, g_2 = C^2, g_{\underline{1}} = \sigma_{diag}C = \sigma_{axis}$, where C is a rotation by $\pi/2$. In the $\underline{112}$ example worked out above, this yields $g_{\underline{1}12} = g_2g_1g_{\underline{1}} = C^2C\sigma_{axis} = \sigma_{diag}$, listed in the last column of table 6. Our convention is to multiply group elements in the reverse order with

respect to the symbol sequence. We need these group elements for our next step, the zeta function factorizations.

The C_{4v} group has four one-dimensional representations, either symmetric (A_1) or antisymmetric (A_2) under both types of reflections, or symmetric under one and antisymmetric under the other (B_1, B_2), and a degenerate pair of two-dimensional representations E . Substituting the C_{4v} characters

C_{4v}	A_1	A_2	B_1	B_2	E
e	1	1	1	1	2
C_2	1	1	1	1	-2
C_4, C_4^3	1	1	-1	-1	0
σ_{axes}	1	-1	1	-1	0
σ_{diag}	1	-1	-1	1	0

into (39) we obtain:

$$\begin{array}{rcccl}
h_{\bar{p}} & & A_1 & A_2 & B_1 & B_2 & E \\
e: & (1 - t_{\bar{p}})^8 & = & (1 - t_{\bar{p}}) & (1 - t_{\bar{p}}) & (1 - t_{\bar{p}}) & (1 - t_{\bar{p}})^4 \\
C_2: & (1 - t_{\bar{p}}^2)^4 & = & (1 - t_{\bar{p}}) & (1 - t_{\bar{p}}) & (1 - t_{\bar{p}}) & (1 + t_{\bar{p}})^4 \\
C_4, C_4^3: & (1 - t_{\bar{p}}^4)^2 & = & (1 - t_{\bar{p}}) & (1 - t_{\bar{p}}) & (1 + t_{\bar{p}}) & (1 + t_{\bar{p}})^2 \\
\sigma_{axes}: & (1 - t_{\bar{p}}^2)^4 & = & (1 - t_{\bar{p}}) & (1 + t_{\bar{p}}) & (1 - t_{\bar{p}}) & (1 - t_{\bar{p}}^2)^2 \\
\sigma_{diag}: & (1 - t_{\bar{p}}^2)^4 & = & (1 - t_{\bar{p}}) & (1 + t_{\bar{p}}) & (1 + t_{\bar{p}}) & (1 - t_{\bar{p}}^2)^2
\end{array}$$

The possible irreducible segment group elements $\mathbf{h}_{\bar{p}}$ are listed in the first column; σ_{axes} denotes a reflection across either the x-axis or the y-axis, and σ_{diag} denotes a reflection across a diagonal (see fig. 4). In addition, degenerate pairs of boundary orbits can run along the symmetry lines in the full space, with the fundamental domain group theory weights $\mathbf{h}_p = (C_2 + \sigma_x)/2$ (axes) and $\mathbf{h}_p = (C_2 + \sigma_{13})/2$ (diagonals) respectively:

$$\begin{array}{rcccl}
& & A_1 & A_2 & B_1 & B_2 & E \\
axes: & (1 - t_{\bar{p}}^2)^2 & = & (1 - t_{\bar{p}})(1 - 0t_{\bar{p}})(1 - t_{\bar{p}})(1 - 0t_{\bar{p}})(1 + t_{\bar{p}})^2 \\
diagonals: & (1 - t_{\bar{p}}^2)^2 & = & (1 - t_{\bar{p}})(1 - 0t_{\bar{p}})(1 - 0t_{\bar{p}})(1 - t_{\bar{p}})(1 + t_{\bar{p}})^2 & (53)
\end{array}$$

(we have assumed that $t_{\bar{p}}$ does not change sign under reflections across symmetry axes). For the 4-disk arrangement considered here only the diagonal orbits $\overline{13}, \overline{24}$ occur; they correspond to the $\overline{2}$ fixed point in the fundamental domain.

The A_1 subspace in C_{4v} cycle expansion is given by

$$\begin{aligned}
1/\zeta_{A_1} &= (1-t_0)(1-t_1)(1-t_2)(1-t_{01})(1-t_{02})(1-t_{12}) \\
&\quad (1-t_{001})(1-t_{002})(1-t_{011})(1-t_{012})(1-t_{021})(1-t_{022})(1-t_{112}) \\
&\quad (1-t_{122})(1-t_{0001})(1-t_{0002})(1-t_{0011})(1-t_{0012})(1-t_{0021}) \dots \\
&= 1-t_0-t_1-t_2-(t_{01}-t_0t_1)-(t_{02}-t_0t_2)-(t_{12}-t_1t_2) \\
&\quad -(t_{001}-t_0t_{01})-(t_{002}-t_0t_{02})-(t_{011}-t_1t_{01}) \\
&\quad -(t_{022}-t_2t_{02})-(t_{112}-t_1t_{12})-(t_{122}-t_2t_{12}) \\
&\quad -(t_{012}+t_{021}+t_0t_1t_2-t_0t_{12}-t_1t_{02}-t_2t_{01}) \dots
\end{aligned} \tag{54}$$

(for typographical convenience, $\underline{1}$ is replaced by 0 in the remainder of this section). For one-dimensional representations, the characters can be read off [63] the symbol strings: $\chi_{A_2}(\mathbf{h}_{\tilde{\mathbf{p}}}) = (-1)^{n_0}$, $\chi_{B_1}(\mathbf{h}_{\tilde{\mathbf{p}}}) = (-1)^{n_1}$, $\chi_{B_2}(\mathbf{h}_{\tilde{\mathbf{p}}}) = (-1)^{n_0+n_1}$, where n_0 and n_1 are the number of times symbols 0, 1 appear in the \tilde{p} symbol string. For B_2 all t_p with an odd total number of 0's and 1's change sign:

$$\begin{aligned}
1/\zeta_{B_2} &= (1+t_0)(1+t_1)(1-t_2)(1-t_{01})(1+t_{02})(1+t_{12}) \\
&\quad (1+t_{001})(1-t_{002})(1+t_{011})(1-t_{012})(1-t_{021})(1+t_{022})(1-t_{112}) \\
&\quad (1+t_{122})(1-t_{0001})(1+t_{0002})(1-t_{0011})(1+t_{0012})(1+t_{0021}) \dots \\
&= 1+t_0+t_1-t_2-(t_{01}-t_0t_1)+(t_{02}-t_0t_2)+(t_{12}-t_1t_2) \\
&\quad +(t_{001}-t_0t_{01})-(t_{002}-t_0t_{02})+(t_{011}-t_1t_{01}) \\
&\quad +(t_{022}-t_2t_{02})-(t_{112}-t_1t_{12})+(t_{122}-t_2t_{12}) \\
&\quad -(t_{012}+t_{021}+t_0t_1t_2-t_0t_{12}-t_1t_{02}-t_2t_{01}) \dots
\end{aligned} \tag{55}$$

The form of the remaining cycle expansions depends crucially on the special role played by the boundary orbits: by (53) the orbit t_2 does not contribute to A_2 and B_1 ,

$$\begin{aligned}
1/\zeta_{A_2} &= (1+t_0)(1-t_1)(1+t_{01})(1+t_{02})(1-t_{12}) \\
&\quad (1-t_{001})(1-t_{002})(1+t_{011})(1+t_{012})(1+t_{021})(1+t_{022})(1-t_{112}) \\
&\quad (1-t_{122})(1+t_{0001})(1+t_{0002})(1-t_{0011})(1-t_{0012})(1-t_{0021}) \dots \\
&= 1+t_0-t_1+(t_{01}-t_0t_1)+t_{02}-t_{12} \\
&\quad -(t_{001}-t_0t_{01})-(t_{002}-t_0t_{02})+(t_{011}+t_1t_{01}) \\
&\quad +t_{022}-t_{122}-(t_{112}-t_1t_{12})+(t_{012}+t_{021}-t_0t_{12}-t_1t_{02}) \dots
\end{aligned} \tag{56}$$

and

$$\begin{aligned}
1/\zeta_{B_1} &= (1-t_0)(1+t_1)(1+t_{01})(1-t_{02})(1+t_{12}) \\
&\quad (1+t_{001})(1-t_{002})(1-t_{011})(1+t_{012})(1+t_{021})(1-t_{022})(1-t_{112}) \\
&\quad (1+t_{122})(1+t_{0001})(1-t_{0002})(1-t_{0011})(1+t_{0012})(1+t_{0021}) \dots \\
&= 1-t_0+t_1+(t_{01}-t_0t_1)-t_{02}+t_{12} \\
&\quad +(t_{001}-t_0t_{01})-(t_{002}-t_0t_{02})-(t_{011}-t_1t_{01}) \\
&\quad -t_{022}+t_{122}-(t_{112}-t_1t_{12})+(t_{012}+t_{021}-t_0t_{12}-t_1t_{02}) \dots \quad (57)
\end{aligned}$$

In the above we have assumed that t_2 does not change sign under C_{4v} reflections. For the mixed-symmetry subspace E the curvature expansion is given by

$$\begin{aligned}
1/\zeta_E &= 1+t_2+(-t_0^2+t_1^2)+(2t_{002}-t_2t_0^2-2t_{112}+t_2t_1^2) \\
&\quad +(2t_{0011}-2t_{0022}+2t_2t_{002}-t_{01}^2-t_{02}^2+2t_{1122}-2t_2t_{112} \\
&\quad +t_{12}^2-t_0^2t_1^2)+(2t_{00002}-2t_{00112}+2t_2t_{0011}-2t_{00121}-2t_{00211} \\
&\quad +2t_{00222}-2t_2t_{0022}+2t_{01012}+2t_{01021}-2t_{01102}-t_2t_{01}^2+2t_{02022} \\
&\quad -t_2t_{02}^2+2t_{11112}-2t_{11222}+2t_2t_{1122}-2t_{12122}+t_2t_{12}^2-t_2t_0^2t_1^2 \\
&\quad +2t_{002}(-t_0^2+t_1^2)-2t_{112}(-t_0^2+t_1^2)) \quad (58)
\end{aligned}$$

A quick test of the $\zeta = \zeta_{A_1}\zeta_{A_2}\zeta_{B_1}\zeta_{B_2}\zeta_E^2$ factorization is afforded by the topological polynomial; substituting $t_p = z^{n_p}$ into the expansion yields

$$1/\zeta_{A_1} = 1 - 3z, \quad 1/\zeta_{A_2} = 1/\zeta_{B_1} = 1, \quad 1/\zeta_{B_2} = 1/\zeta_E = 1 + z,$$

in agreement with (23).

7.4 C_{2v} factorization

An arrangement of four identical disks on the vertices of a rectangle has C_{2v} symmetry (fig.5). C_{2v} consists of $\{e, \sigma_x, \sigma_y, C_2\}$, *i.e.*, the reflections across the symmetry axes and a rotation by π . C_{2v} is the symmetry of several systems studied in the literature, such as the stadium billiard[49], and the 2-dimensional anisotropic Kepler potential[24].

This system affords a rather easy visualisation of the conversion of a 4-disk dynamics into a fundamental domain symbolic dynamics. An orbit leaving the fundamental domain through one of the axis may be folded back by a reflection

on that axis; with these symmetry operations $g_0 = \sigma_x$ and $g_1 = \sigma_y$ we associate labels 1 and 0, respectively. Orbits going to the diagonally opposed disk cross the boundaries of the fundamental domain twice; the product of these two reflections is just $C_2 = \sigma_x \sigma_y$, to which we assign the label 2. For example, a ternary string $0010201\dots$ is converted into $12143123\dots$, and the associated group-theory weight is given by $\dots g_1 g_0 g_2 g_0 g_1 g_0 g_0$.

Short ternary cycles and the corresponding 4-disk cycles are listed in table 7. Note that already at length three there is a pair of cycles ($012 = 143$ and $021 = 142$) related by time reversal, but *not* by any C_{2v} symmetries.

The above is the complete description of the symbolic dynamics for 4 sufficiently separated equal disks placed at corners of a rectangle. However, if the fundamental domain requires further partitioning, the ternary description is insufficient. For example, in the stadium billiard fundamental domain one has to distinguish between bounces off the straight and the curved sections of the billiard wall; in that case there exists evidence[64] that five symbols suffice for constructing the covering symbolic dynamics.

The group C_{2v} has four one-dimensional representations, distinguished by their behaviour under axis reflections. The A_1 representation is symmetric with respect to both reflections; the A_2 representation is antisymmetric with respect to both. The B_1 and B_2 representations are symmetric under one and antisymmetric under the other reflection. The character table is

C_{2v}	A_1	A_2	B_1	B_2
e	1	1	1	1
C_2	1	1	-1	-1
σ_x	1	-1	1	-1
σ_y	1	-1	-1	1

Substituted into the factorized determinant (38), the contributions of periodic orbits split as follows

$$\begin{array}{l}
g_{\bar{p}} \\
e: (1 - t_{\bar{p}})^4 = (1 - t_{\bar{p}}) (1 - t_{\bar{p}}) (1 - t_{\bar{p}}) (1 - t_{\bar{p}}) \\
C_2: (1 - t_{\bar{p}}^2)^2 = (1 - t_{\bar{p}}) (1 - t_{\bar{p}}) (1 - t_{\bar{p}}) (1 - t_{\bar{p}}) \\
\sigma_x: (1 - t_{\bar{p}}^2)^2 = (1 - t_{\bar{p}}) (1 + t_{\bar{p}}) (1 - t_{\bar{p}}) (1 + t_{\bar{p}}) \\
\sigma_y: (1 - t_{\bar{p}}^2)^2 = (1 - t_{\bar{p}}) (1 + t_{\bar{p}}) (1 + t_{\bar{p}}) (1 - t_{\bar{p}})
\end{array}$$

Cycle expansions follow by substituting cycles and their group theory factors from table 7. For A_1 all characters are +1, and the corresponding cycle expansion is given in (54). Similarly, the totally antisymmetric subspace factorization A_2 is given by (55), the B_2 factorization of C_{4v} . For B_1 all t_p with an odd total number of 0's and 2's change sign:

$$\begin{aligned}
1/\zeta_{B_1} &= (1+t_0)(1-t_1)(1+t_2)(1+t_{01})(1-t_{02})(1+t_{12}) \\
&\quad (1-t_{001})(1+t_{002})(1+t_{011})(1-t_{012})(1-t_{021})(1+t_{022})(1+t_{112}) \\
&\quad (1-t_{122})(1+t_{0001})(1-t_{0002})(1-t_{0011})(1+t_{0012})(1+t_{0021}) \dots \\
&= 1+t_0-t_1+t_2+(t_{01}-t_0t_1)-(t_{02}-t_0t_2)+(t_{12}-t_1t_2) \\
&\quad -(t_{001}-t_0t_{01})+(t_{002}-t_0t_{02})+(t_{011}-t_1t_{01}) \\
&\quad +(t_{022}-t_2t_{02})+(t_{112}-t_1t_{12})-(t_{122}-t_2t_{12}) \\
&\quad -(t_{012}+t_{021}+t_0t_1t_2-t_0t_{12}-t_1t_{02}-t_2t_{01}) \dots
\end{aligned} \tag{59}$$

For B_2 all t_p with an odd total number of 1's and 2's change sign:

$$\begin{aligned}
1/\zeta_{B_2} &= (1-t_0)(1+t_1)(1+t_2)(1+t_{01})(1+t_{02})(1-t_{12}) \\
&\quad (1+t_{001})(1+t_{002})(1-t_{011})(1-t_{012})(1-t_{021})(1-t_{022})(1+t_{112}) \\
&\quad (1+t_{122})(1+t_{0001})(1+t_{0002})(1-t_{0011})(1-t_{0012})(1-t_{0021}) \dots \\
&= 1-t_0+t_1+t_2+(t_{01}-t_0t_1)+(t_{02}-t_0t_2)-(t_{12}-t_1t_2) \\
&\quad +(t_{001}-t_0t_{01})+(t_{002}-t_0t_{02})-(t_{011}-t_1t_{01}) \\
&\quad -(t_{022}-t_2t_{02})+(t_{112}-t_1t_{12})+(t_{122}-t_2t_{12}) \\
&\quad -(t_{012}+t_{021}+t_0t_1t_2-t_0t_{12}-t_1t_{02}-t_2t_{01}) \dots
\end{aligned} \tag{60}$$

Note that all of the above cycle expansions group long orbits together with their pseudo-orbit shadows, so that the shadowing arguments for convergence[18] still apply.

The topological polynomial factorizes as

$$\frac{1}{\zeta_{A_1}} = 1 - 3z \quad , \quad \frac{1}{\zeta_{A_2}} = \frac{1}{\zeta_{B_1}} = \frac{1}{\zeta_{B_2}} = 1 + z,$$

consistent with the 4-disk factorization (23).

8 Summary

The techniques of this paper have been applied to computations of the 3-disk classical and quantum spectra in refs. [46, 42, 50], and to a ‘‘Zeeman effect’’ pinball

and the x^2y^2 potentials in refs. [22, 63]. The main lesson of such calculations is that if a dynamical system has a discrete symmetry, the symmetry should be exploited; much is gained, both in understanding of the spectra and ease of their evaluation. Once this is appreciated, it is hard to conceive of a calculation without factorization; it would correspond to quantum mechanical calculations without wave-function symmetrizations.

In a larger perspective, the factorizations developed above are special cases of a general approach to exploiting the group-theoretic invariances in spectra computations, such as those used in enumeration of periodic geodesics[27, 65, 41] for hyperbolic billiards[10, 13] and Selberg zeta functions[14].

Reduction to the fundamental domain simplifies symbolic dynamics and eliminates symmetry induced degeneracies. While the resummation of the theory from the trace sums[12] to the cycle expansions[53] does not reduce the exponential growth in number of cycles with the cycle length, in practice only the short orbits are used, and for them the labor saving is dramatic. For example, for the 3-disk pinball there are 256 periodic points of length 8, but reduction to the fundamental domain non-degenerate prime cycles reduces the number of the distinct cycles of length 8 to 30.

In addition, as we demonstrate by explicit calculations in ref. [9, 42], cycle expansions of the symmetry reduced zeta functions converge dramatically faster than the unfactorized zeta functions. One reason is that the unfactorized zeta function has many closely spaced zeros and zeros of multiplicity higher than one; since the cycle expansion is a polynomial expansion in topological cycle length, accomodating such behaviour requires many terms. The zeta functions on separate subspaces have more evenly and widely spaced zeros, are smoother, do not have symmetry-induced multiple zeros, and fewer cycle expansion terms (short cycle truncations) suffice to determine them. Furthermore, the cycles in the fundamental domain sample phase space more densely than in the full space. For example, for the 3-disk problem, there are 9 distinct (symmetry unrelated) cycles of length 7 or less in full space, corresponding to 47 distinct periodic points. In the fundamental domain, we have 8 (distinct) periodic orbits up to length 4 and thus 22 different periodic points in 1/6-th the phase space, *i.e.*, an increase in density by a factor 3 with the same numerical effort.

We emphasize that the symmetry factorization (49) of the dynamical zeta function is *intrinsic* to the classical dynamics, and not a special property of quantal

spectra (in which context it was used before[23]). Our results are not restricted to the Hamiltonian systems, or only to the configuration space symmetries; for example, the discrete symmetry can be a symmetry of the Hamiltonian phase space[25]. In conclusion, the manifold advantages of the symmetry reduced dynamics should thus be obvious; full space cycle expansions, such as those included in the appendix, are useful only for cross checking purposes.

9 Appendix

Here we list the 3- and 4-disk cycle expansions for unfactorized zeta functions. They are not recommended for actual computations, as the factorized zeta functions yield much better spectra, but they might be useful for cross-checking purposes.

For the 3-disk pinball (assuming no symmetries between disks) the curvature expansion (5) is given by:

$$\begin{aligned}
1/\zeta &= (1 - z^2 t_{12})(1 - z^2 t_{13})(1 - z^2 t_{23})(1 - z^3 t_{123})(1 - z^3 t_{132}) \\
&\quad (1 - z^4 t_{1213})(1 - z^4 t_{1232})(1 - z^4 t_{1323})(1 - z^5 t_{12123}) \dots \\
&= 1 - z^2 t_{12} - z^2 t_{23} - z^2 t_{31} - z^3 t_{123} - z^3 t_{132} \\
&\quad - z^4 [(t_{1213} - t_{12}t_{13}) + (t_{1232} - t_{12}t_{23}) + (t_{1323} - t_{13}t_{23})] \\
&\quad - z^5 [(t_{12123} - t_{12}t_{123}) + \dots] - \dots
\end{aligned} \tag{61}$$

The symmetrically arranged 3-disk pinball cycle expansion of the Euler product (30) (see table 2 and fig.1) is given by:

$$\begin{aligned}
1/\zeta &= (1 - z^2 t_{12})^3 (1 - z^3 t_{123})^2 (1 - z^4 t_{1213})^3 \\
&\quad (1 - z^5 t_{12123})^6 (1 - z^6 t_{121213})^6 (1 - z^6 t_{121323})^3 \dots \\
&= 1 - 3z^2 t_{12} - 2z^3 t_{123} - 3z^4 (t_{1213} - t_{12}^2) - 6z^5 (t_{12123} - t_{12}t_{123}) \\
&\quad - z^6 (6t_{121213} + 3t_{121323} + t_{12}^3 - 9t_{12}t_{1213} - t_{123}^2) \\
&\quad - 6z^7 (t_{1212123} + t_{1212313} + t_{1213123} + t_{12}^2 t_{123} - 3t_{12}t_{12123} - t_{123}t_{1213}) \\
&\quad - 3z^8 (2t_{12121213} + t_{12121313} + 2t_{12121323} + 2t_{12123123} \\
&\quad + 2t_{12123213} + t_{12132123} + 3t_{12}^2 t_{1213} + t_{12}t_{123}^2 \\
&\quad - 6t_{12}t_{121213} - 3t_{12}t_{121323} - 4t_{123}t_{12123} - t_{1213}^2) - \dots
\end{aligned} \tag{62}$$

For the symmetricly arranged 4-disk pinball the symmetry group is C_{4v} , of order

8. The degenerate cycles can have multiplicities 2, 4 or 8 (see table 3):

$$\begin{aligned}
1/\zeta = & (1 - z^2 t_{12})^4 (1 - z^2 t_{13})^2 (1 - z^3 t_{123})^8 (1 - z^4 t_{1213})^8 (1 - z^4 t_{1214})^4 \\
& (1 - z^4 t_{1234})^2 (1 - z^4 t_{1243})^4 (1 - z^5 t_{12123})^8 (1 - z^5 t_{12124})^8 (1 - z^5 t_{12134})^8 \\
& (1 - z^5 t_{12143})^8 (1 - z^5 t_{12313})^8 (1 - z^5 t_{12413})^8 \dots
\end{aligned} \tag{63}$$

and the cycle expansion is given by

$$\begin{aligned}
1/\zeta = & 1 - z^2(4 t_{12} + 2 t_{13}) - 8z^3 t_{123} \\
& - z^4(8 t_{1213} + 4 t_{1214} + 2 t_{1234} + 4 t_{1243} - 6 t_{12}^2 - t_{13}^2 - 8 t_{12} t_{13}) \\
& - 8z^5(t_{12123} + t_{12124} + t_{12134} + t_{12143} + t_{12313} + t_{12413} - 4 t_{12} t_{123} - 2 t_{13} t_{123}) \\
& - 4z^6(2 S_8 + S_4 + t_{12}^3 + 3 t_{12}^2 t_{13} + t_{12} t_{13}^2 - 8 t_{12} t_{1213} - 4 t_{12} t_{1214} \\
& - 2 t_{12} t_{1234} - 4 t_{12} t_{1243} - 4 t_{13} t_{1213} - 2 t_{13} t_{1214} - t_{13} t_{1234} \\
& - 2 t_{13} t_{1243} - 7 t_{123}^2) - \dots
\end{aligned} \tag{64}$$

where in the coefficient to z^6 the abbreviations S_8 and S_4 stand for the sums over the weights of the 12 orbits with multiplicity 8 and the 5 orbits of multiplicity 4, respectively; the orbits are listed in table 2.

Acknowledgements

We are grateful to the hospitality of the Max Planck Institut für Mathematik, during whose spring 1988 Chaos and Fractals workshop this collaboration was initiated. We acknowledge stimulating exchanges with F. Christiansen, P. Dahlqvist, G. Eilenberger, P. Grassberger, M. Gutzwiller, K.T. Hansen, T. Janssen, B. Lautritzen, G. Ott, J.M. Robbins, H.H. Rugh, G. Russberg, M. Sieber, and D. Wintgen. P.C. is grateful to the Carlsberg Foundation for support, to I. Procaccia of the Weizmann Institute, P. Hemmer of University of Trondheim and J. Lowenstein of New York University, where parts of this work were done, for the hospitality. B.E. was supported in part by the National Science Foundation under Grant No. PHY82-17853, supplemented by funds from the National Aeronautics and Space Administration.

References

- [1] H. Poincaré, *Les méthodes nouvelles de la mécanique céleste* (Guthier-Villars, Paris 1892-99)
- [2] S. Smale, *Bull. Am. Math. Soc.* **73**, 747 (1967)
- [3] Ya. G. Sinai, *Russ. Math. Surveys* **166**, 21 (1972)
- [4] R. Bowen, *Equilibrium states and the ergodic theory of Anosov-diffeomorphisms*, Springer Lecture Notes in Math. **470** (1975)
- [5] D. Ruelle, *Statistical Mechanics*, (Addison-Wesley, Reading 1978)
- [6] C. Grebogi, E. Ott and J.A. Yorke, *Phys. Rev. A* **36**, 3522 (1987)
- [7] P. Cvitanović, G.H. Gunaratne and I. Procaccia, *Phys. Rev. A* **38**, 1503 (1988)
- [8] G.H. Gunaratne, M.H. Jensen and I. Procaccia, *Nonlinearity* **1**, 157 (1988)
- [9] P. Cvitanović and B. Eckhardt, *Phys. Rev. Lett.* **63**, 823 (1989)
- [10] J. Hadamard, *J. Math. Pure Appl.* **4**, 27 (1898)
- [11] A. Selberg, *J. Ind. Math. Soc.* **20**, 47 (1956)
- [12] M.C. Gutzwiller, *J. Phys. Chem.* **92**, 3154 (1984)
- [13] M.C. Gutzwiller, *J. Math. Phys.* **8**, 1979 (1967); **10**, 1004 (1969); **11**, 1791 (1970); **12**, 343 (1971)
- [14] M.C. Gutzwiller, *Chaos in Classical and Quantum Mechanics* (Springer, New York 1990)
- [15] R. Balian and C. Bloch, *Ann. Phys. (NY)* **85**, 514 (1974)
- [16] M.V. Berry, in *Chaotic Behaviour in Deterministic Systems*, G. Iooss, R.H.G. Helleman and R. Stora, eds., pp. 171–271 (North Holland, Amsterdam 1983)
- [17] A. Voros, *J. Phys.* **A 21**, 685 (1988)
- [18] R. Artuso, E. Aurell and P. Cvitanović, *Nonlinearity* **3**, 325 (1990)
- [19] R. Artuso, E. Aurell and P. Cvitanović, *Nonlinearity* **3**, 361 (1990)
- [20] F. Christiansen, G. Paladin and H.H. Rugh, *Phys. Rev. Lett.* **65**, 2087 (1990)
- [21] F. Christiansen, P. Cvitanović and H.H. Rugh, *J. Phys.* **A 23**, L713 (1990)
- [22] G. Russberg, (in preparation)
- [23] P. Gaspard and S. Rice, *J. Chem. Phys.* **90**, 2225 (1989); **90**, 2242 (1989); **90**, 2255 (1989)
- [24] M.C. Gutzwiller, *Physica D* **5**, 183 (1982)
- [25] J.M. Robbins, *Phys. Rev. A* **40**, 2128 (1989)
- [26] B. Lauritzen, *Phys. Rev. A* **43**, 603 (1991)
- [27] N. Balasz and A. Voros, *Phys. Rep.* **143**, 109 (1986)

- [28] E. N. Lorenz, *J. Atmospheric Phys.* **20**, 130 (1963)
- [29] G. Ott and G. Eilenberger, private communication.
- [30] G. Tanner and D. Wintgen, *CHAOS* **2**, 53 (1992).
- [31] P. Cvitanović and F. Christiansen, *CHAOS* **2**, 61 (1992).
- [32] M. Henón and C. Heiles, *J. Astron.* **69**, 73 (1964)
- [33] C. Jung and H.J. Scholz, *J. Phys.* **A 20**, 3607 (1987)
- [34] C. Jung and P. Richter, *J. Phys.* **A 23**, 2847 (1990)
- [35] B. Eckhardt, G. Hose and E. Pollak, *Phys. Rev.* **A 39**, 3776 (1989)
- [36] C. C. Martens, R. L. Waterland, and W. P. Reinhardt, *J. Chem. Phys.* **90**, 2328 (1989)
- [37] S.G. Matanyan, G.K. Savvidy, and N.G. Ter-Arutyunyan-Savvidy, *Sov. Phys. JETP* **53**, 421 (1981)
- [38] A. Carnegie and I. C. Percival, *J. Phys.* **A 17**, 801 (1984)
- [39] B. Eckhardt and D. Wintgen, *J. Phys.* **B 23**, 355 (1990)
- [40] B. Eckhardt, *J. Phys.* **A 20**, 5971 (1987)
- [41] M. Sieber and F. Steiner, *Phys. Lett.* **A 148**, 415 (1990)
- [42] B. Eckhardt, G. Russberg, P. Cvitanović, P.E. Rosenqvist, and P. Scherer, in G. Casati and B. Chirikov, eds., *Quantum Chaos* (Cambridge University Press, Cambridge 1993)
- [43] B. Eckhardt and D. Wintgen, *J. Phys.* **A 24**, 4335 (1991)
- [44] P. Dahlqvist and G. Russberg, *Phys. Rev. Lett.* **65**, 2837 (1990)
- [45] L. Kadanoff and C. Tang, *Proc. Natl. Acad. Sci. USA* **81**, 1276 (1984)
- [46] P. Cvitanović and B. Eckhardt, *J. Phys.* **A 24**, L237 (1991)
- [47] P. Cvitanović, *Physica* **D 51**, 138 (1991).
- [48] P. Grassberger, F. Christiansen and H.H. Rugh (private communications)
- [49] L. Bunimovich, *Funkts. Anal. Ego Prilozh.* **8**, 73 (1974); *Comm. Math. Phys.* **65**, 295 (1979)
- [50] P. Scherer, Ph.D. thesis, Köln 1991
- [51] K.T. Hansen, *CHAOS* **2**, 71 (1992); *Nonlinearity* to appear.
- [52] G. D'Alessandro, P. Grassberger, S. Isola and A. Politi, *J. Phys.* **A 23**, 5285 (1990)
- [53] P. Cvitanović, *Phys. Rev. Lett.* **61**, 2729 (1988)
- [54] See for example G. M. Hardy and E. M. Wright, *The Theory of Numbers*, (Oxford Univ. Press, Oxford 1938)
- [55] E. Artin and B. Mazur, *Ann. Math.* **81**, 82 (1965)

- [56] M. Hamermesh, *Group Theory and its Application to Physical Problems* (Addison-Wesley, Reading, 1962)
- [57] F. Christiansen, Master's Thesis, Univ. of Copenhagen (June 1989)
- [58] M. Hénon, *Physica D* **5**, 412 (1982)
- [59] R. DeVogelaere, in *Contributions to the theory of nonlinear oscillations*, S. Lefschetz, ed, pp. 54–84 (Princeton University Press, Princeton 1958).
- [60] A. Hönig and D. Wintgen, *Phys. Rev. A* **39**, 5642 (1989)
- [61] B. Eckhardt, *Symmetries and Spectra of Maps*, submitted to *Acta Phys. Pol.*
- [62] R. Mainieri, Ph. D. thesis, New York University (Aug 1990); *Phys. Rev. A* **45**, 3580 (1992)
- [63] P. Dahlqvist and G. Russberg, *J. Phys. A* **24**, 4763 (1991)
- [64] O. Biham and M. Kvale, *Phys. Rev. A* **46**, 6334 (1992); K.T. Hansen, *Nonlinearity* to appear.
- [65] see for ex. A. Terras, *Harmonic Analysis on Symmetric Spaces and Applications I* (Springer, Berlin 1985); H.P. McKean, *Comm. Pure & Appl. Math.*, **25**, 225 (1972); **27**, 134 (1974)

Figure captions

1. The symmetries of three disks on an equilateral triangle. The fundamental domain is indicated by the shaded wedge.
2. Some examples of 3-disk cycles. (a) $\overline{12123}$ and $\overline{13132}$ are mapped into each other by σ_{23} , the flip across 1 axis; this orbit has degeneracy 6 under C_{3v} symmetries. Similarly (b) $\overline{123}$ and $\overline{132}$ and (c) $\overline{1213}$, $\overline{1232}$ and $\overline{1323}$ are degenerate under C_{3v} . The orbits (d) $\overline{121212313}$ and $\overline{121212323}$ are related by time reversal but not by any C_{3v} symmetry.
3. The scattering geometry for the disk radius/separation ratio $a : R = 1 : 2.5$. (a) the three disks, with $\overline{12}$, $\overline{123}$ and $\overline{121232313}$ cycles indicated. (b) the fundamental domain, *ie.* a wedge consisting of a section of a disk, two segments of symmetry axes acting as straight mirror walls, and an escape gap. The above cycles restricted to the fundamental domain are now the two fixed points $\overline{0}$ and $\overline{1}$ and the $\overline{100}$ cycle.
4. The symmetries of four disks on a square. The fundamental domain is indicated by the shaded wedge.
5. The symmetries of four disks on a rectangle. The fundamental domain is indicated by the shaded wedge.

n	M_n	N_n	S_n	$m_p \cdot \hat{p}$
1	0	0	0	
2	3	6=3·2	1	3·12
3	2	6=2·3	1	2·123
4	3	18=3·2+3·4	1	3·1213
5	6	30=6·5	1	6·12123
6	9	66=3·2+2·3+9·6	2	6·121213 + 3·121323
7	18	126=18·7	3	6·1212123 + 6·1212313 + 6·1213123
8	30	258=3·2+3·4+30·8	6	6·12121213 + 3·12121313 + 6·12121323 + 6·12123123 + 6·12123213 + 3·12132123
9	56	510=2·3+56·9	10	6·121212123 + 6·(121212313 + 121212323) + 6·(121213123 + 121213213) + 6·121231323 + 6·(121231213 + 121232123) + 2·121232313 + 6·121321323
10	99	1022	18	

Table 1. List of the 3-disk prime cycles up to length 10. Here n is the cycle length, M_n the number of prime cycles, N_n the number of periodic points and S_n the number of distinct prime cycles under the C_{3v} symmetry. Column 3 also indicates the splitting of N_n into contributions from orbits of lengths that divide n . The prefactors in the fifth column indicate the degeneracy m_p of the cycle; for example, 3·12 stands for the three prime cycles $\overline{12}$, $\overline{13}$ and $\overline{23}$ related by $2\pi/3$ rotations. Among symmetry related cycles, a representative \hat{p} which is lexically lowest was chosen. The cycles of length 9 grouped by parenthesis are related by time reversal symmetry (but not by any other C_{3v} transformation).

n	M_n	N_n	S_n	$m_p \cdot \hat{p}$
1	0	0	0	
2	6	12=6·2	2	4·12 + 2·13
3	8	24=8·3	1	8·123
4	18	84=6·2+18·4	4	8·1213 + 4·1214 + 2·1234 + 4·1243
5	48	240=48·5	6	8·(12123 + 12124) + 8·12313 + 8·(12134 + 12143) + 8·12413
6	116	732=6·2+8·3+116·6	17	8·121213 + 8·121214 + 8·121234 + 8·121243 + 8·121313 + 8·121314 + 4·121323 + 8·(121324 + 121423) + 4·121343 + 8·121424 + 4·121434 + 8·123124 + 8·123134 + 4·123143 + 4·124213 + 8·124243
7	312	2184	39	
8	810	6564	108	

Table 2. List of the 4-disk prime cycles up to length 8. The meaning of the symbols is the same as in Table 1. Orbits related by time reversal symmetry (but no other symmetry) already appear at cycle length 5. List of the cycles of length 7 and 8 has been omitted.

n	$M_n(N)$	$M_n(2)$	$M_n(3)$	$M_n(4)$
1	N	2	3	4
2	$N(N-1)/2$	1	3	6
3	$N(N^2-1)/3$	2	8	20
4	$N^2(N^2-1)/4$	3	18	60
5	$(N^5-N)/5$	6	48	204
6	$(N^6-N^3-N^2+N)/6$	9	116	670
7	$(N^7-N)/7$	18	312	2340
8	$N^4(N^4-1)/8$	30	810	8160
9	$N^3(N^6-1)/9$	56	2184	29120
10	$(N^{10}-N^5-N^2+N)/10$	99	5880	104754

Table 3. Number of prime cycles for various alphabets and grammars up to length 10. The first column gives the cycle length, the second the formula (11) for the number of prime cycles for complete N -symbol dynamics, columns three through five give the numbers for $N = 2, 3$ and 4.

\tilde{p}	p	m_p
1	+	2
0	-+	1
01	-- ++	1
001	-++	2
011	--- +++	1
0001	-+--+-++	1
0011	-+++	2
0111	---- +++++	1
00001	-+-+-	2
00011	-+----+-+++	1
00101	-++--+-+++	1
00111	-+----+-+++	1
01011	--+++	2
01111	---- +++++	1
001011	-++--+-+++	1
001101	-++++-+-+++	1

Table 4. Correspondence between the C_2 symmetry reduced cycles \tilde{p} and the standard Ising model periodic configurations p , together with their multiplicities m_p . Also listed are the two shortest cycles (length 6) related by time reversal, but distinct under C_2 .

\tilde{p}	p	$\mathbf{g}_{\tilde{p}}$
0	1 2	σ_{12}
1	1 2 3	C_3
01	12 13	σ_{23}
001	121 232 313	C_3
011	121 323	σ_{13}
0001	1212 1313	σ_{23}
0011	1212 3131 2323	C_3^2
0111	1213 2123	σ_{12}
00001	12121 23232 31313	C_3
00011	12121 32323	σ_{13}
00101	12123 21213	σ_{12}
00111	12123	e
01011	12131 23212 31323	C_3
01111	12132 13123	σ_{23}
000001	121212 131313	σ_{23}
000011	121212 313131 232323	C_3^2
000101	121213	e
000111	121213 212123	σ_{12}
001011	121232 131323	σ_{23}
001101	121231 323213	σ_{13}
001111	121231 232312 313123	C_3
010111	121312 313231 232123	C_3^2
011111	121321 323123	σ_{13}

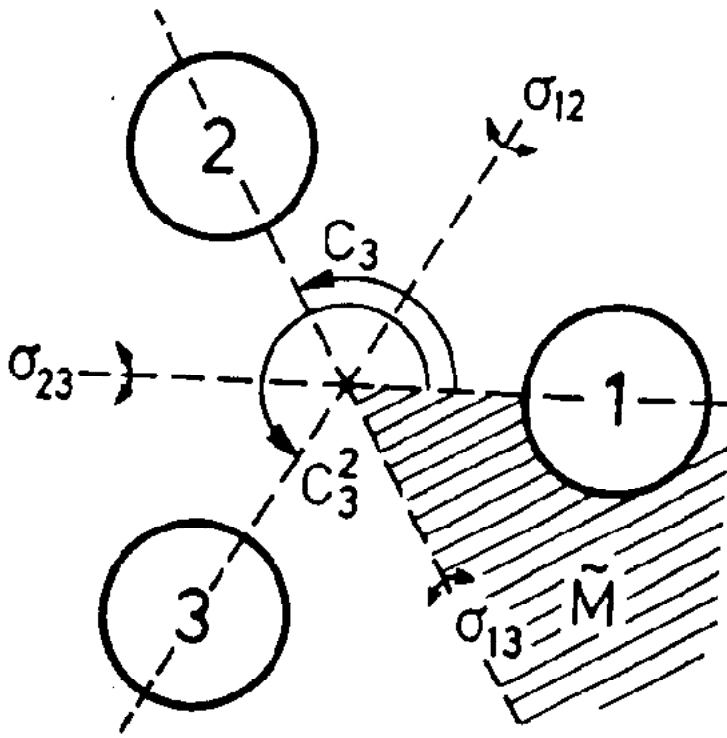
Table 5. C_{3v} correspondence between the binary labelled fundamental domain prime cycles \tilde{p} and the full 3-disk ternary $\{1,2,3\}$ labelled cycles p , together with the C_{3v} transformation that maps the end point of the \tilde{p} cycle into the irreducible segment of the p cycle. The degeneracy of p cycle is $m_p = 6n_{\tilde{p}}/n_p$. The shortest pair of the fundamental domain cycles related by time symmetry are the 6-cycles $\overline{001011}$ and $\overline{001101}$.

\tilde{p}	p	$\mathbf{h}_{\tilde{p}}$
0	1 2	σ_x
1	1 2 3 4	C_4
2	1 3	C_2, σ_{13}
01	12 14	σ_{24}
02	12 43	σ_y
12	12 41 34 23	C_4^3
001	121 232 343 414	C_4
002	121 343	C_2
011	121 434	σ_y
012	121 323	σ_{13}
021	124 324	σ_{13}
022	124 213	σ_x
112	123	e
122	124 231 342 413	C_4
0001	1212 1414	σ_{24}
0002	1212 4343	σ_y
0011	1212 3434	C_2
0012	1212 4141 3434 2323	C_4^3
0021 (a)	1213 4142 3431 2324	C_4^3
0022	1213	e
0102 (a)	1214 2321 3432 4143	C_4
0111	1214 3234	σ_{13}
0112 (b)	1214 2123	σ_x
0121 (b)	1213 2124	σ_x
0122	1213 1413	σ_{24}
0211	1243 2134	σ_x
0212	1243 1423	σ_{24}
0221	1242 1424	σ_{24}
0222	1242 4313	σ_y
1112	1234 2341 3412 4123	C_4
1122	1231 3413	C_2
1222	1242 4131 3424 2313	C_4^3

Table 6. C_{4v} correspondence between the ternary fundamental domain prime cycles \tilde{p} and the full 4-disk $\{1,2,3,4\}$ labelled cycles p , together with the C_{4v} transformation that maps the end point of the \tilde{p} cycle into an irreducible segment of the p cycle. For typographical convenience, the symbol $\underline{1}$ of sect. 7.3 has been replaced by 0, so that the ternary alphabet is $\{0,1,2\}$. The degeneracy of the p cycle is $m_p = 8n_{\tilde{p}}/n_p$. Orbit $\bar{2}$ is the sole boundary orbit, invariant both under a rotation by π and a reflection across a diagonal. The two pairs of cycles marked by (a) and (b) are related by time reversal, but cannot be mapped into each other by C_{4v} transformations.

\tilde{p}	p	\mathbf{g}
0	1 4	σ_y
1	1 2	σ_x
2	1 3	C_2
01	14 32	C_2
02	14 23	σ_x
12	12 43	σ_y
001	141 232	σ_x
002	141 323	C_2
011	143 412	σ_y
012	143	e
021	142	e
022	142 413	σ_y
112	121 343	C_2
122	124 213	σ_x
0001	1414 3232	C_2
0002	1414 2323	σ_x
0011	1412	e
0012	1412 4143	σ_y
0021	1413 4142	σ_y
0022	1413	e
0102	1432 4123	σ_y
0111	1434 3212	C_2
0112	1434 2343	σ_x
0121	1431 2342	σ_x
0122	1431 3213	C_2
0211	1421 2312	σ_x
0212	1421 3243	C_2
0221	1424 3242	C_2
0222	1424 2313	σ_x
1112	1212 4343	σ_y
1122	1213	e
1222	1242 4313	σ_y

Table 7. C_{2v} correspondence between the ternary $\{0, 1, 2\}$ fundamental domain prime cycles \tilde{p} and the full 4-disk $\{1, 2, 3, 4\}$ cycles p , together with the C_{2v} transformation that maps the end point of the \tilde{p} cycle into an irreducible segment of the p cycle. The degeneracy of the p cycle is $m_p = 4n_{\tilde{p}}/n_p$. Note that the 012 and 021 cycles are related by time reversal, but cannot be mapped into each other by C_{2v} transformations. The full space orbit listed here is generated from the symmetry reduced code by the rules given in section 7.4, starting from disk 1.



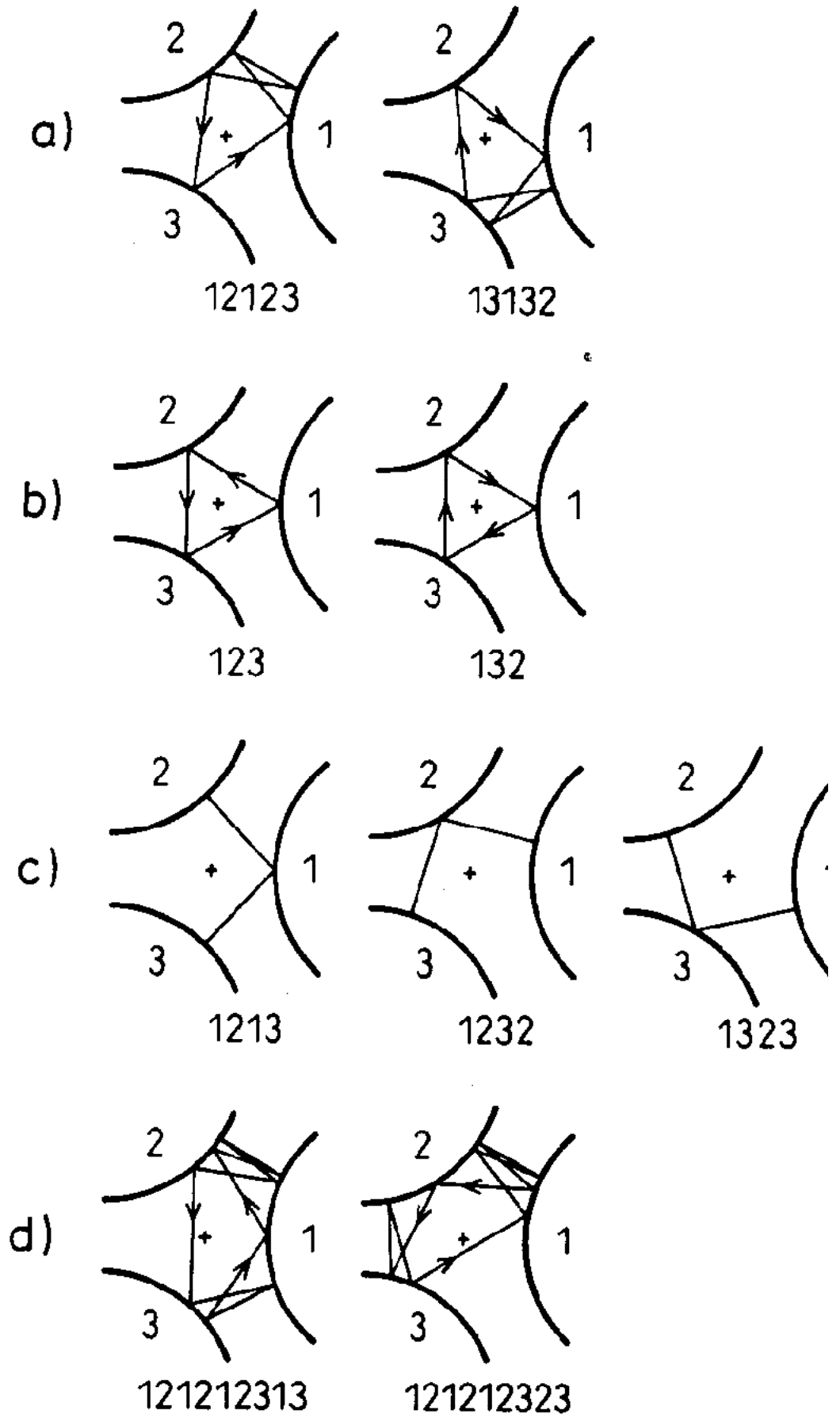
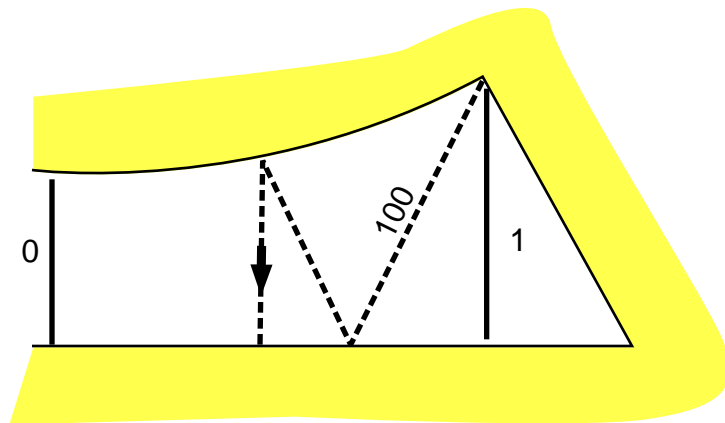
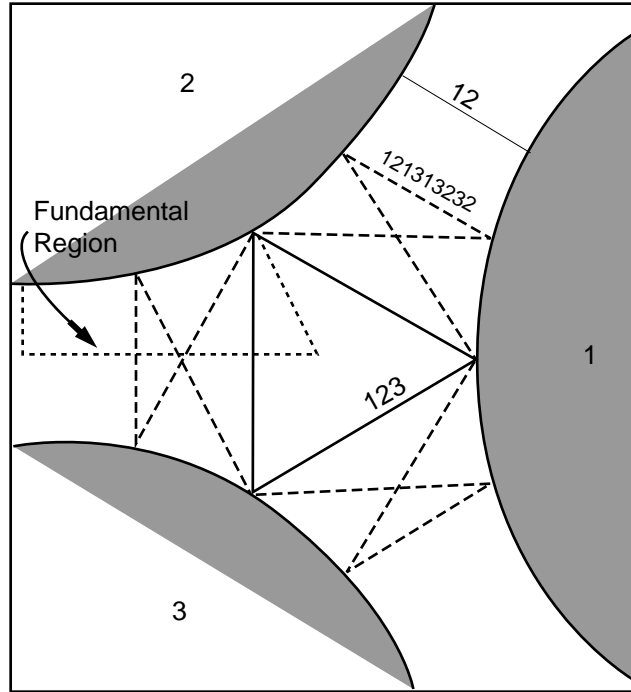


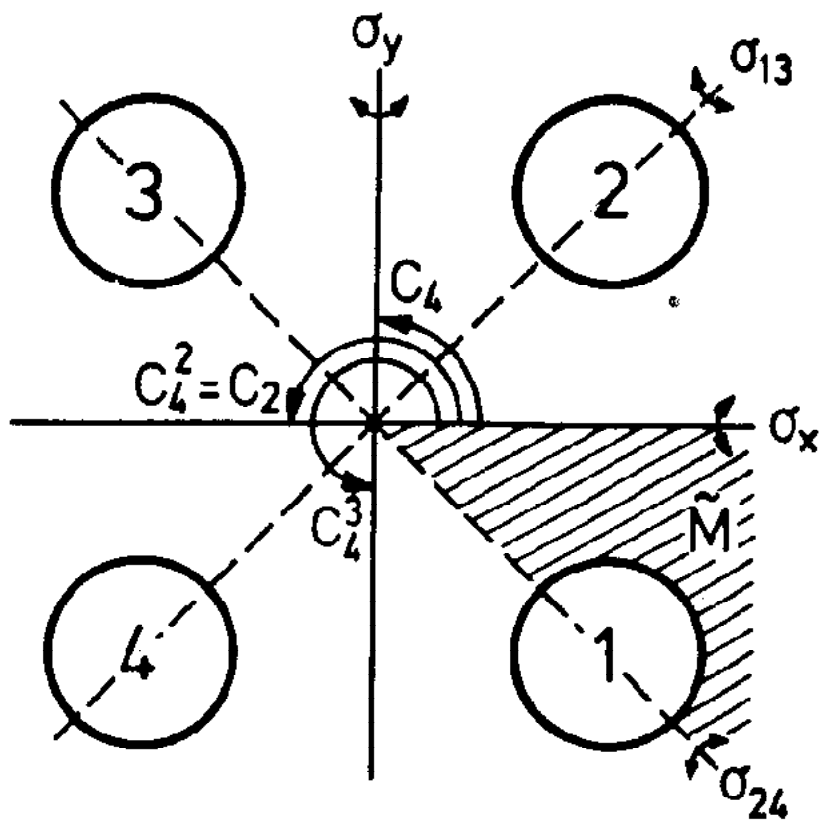
Fig 2

'

1

'





Fig

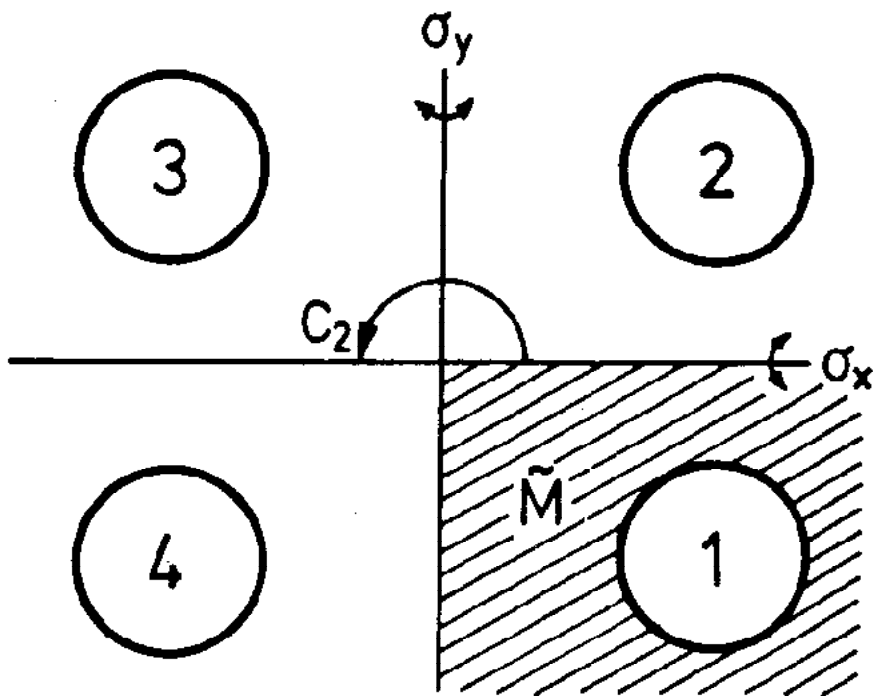


Fig 5

4

